universität wien

MASTERARBEIT / MASTER'S THESIS

Titel der Masterarbeit / Title of the Master's Thesis

Effects of miR-181a knockdown on human dendritic cell differentiation and maturation

verfasst von / submitted by

Johann Romberger, BSc

angestrebter akademischer Grad / in partial fulfillment of the requirements for the degree of

Master of Science (MSc)

Wien, 2016 / Vienna, 2016

Studienkennzahl lt. Studienblatt / degree programme code as it appears on the student record sheet:	A 066 834
Studienrichtung lt. Studienblatt / degree programme as it appears on the student record sheet:	Masterstudium Molekulare Biologie
Betreut von / Supervisor:	Univ.-Prof. Dr.med.univ. Herbert Strobl

Acknowledgement

First, I would like express my sincere gratitude to Prof. Dr. Herbert Strobl for the opportunity of having been able to work on this exciting project as well as for his unparalleled efforts and support for my Master's thesis. Likewise, my outspoken gratitude goes to my supervisor Clarice Lim for sharing her vast knowledge as well as for her patience with me.

I would also like to thank all my fellow labmates and colleagues at the Medical Universities of Vienna and Graz and at the IST Klosterneuburg for their helpfulness during my project as well as for making my stay at the aforementioned institutes great and enjoyable. Special thanks go to Ass. Prof. Gijs Versteeg for kindly providing the SIV plasmid, to Prof. Dr. Timothy Skern, without whom my English would surely still be quite atrocious, as well as to the nurses at the AKH Wien for their friendly help during cord blood acquisition.

Finally, my most cordial thanks go to my parents, family and friends for their invaluable backing and encouragement and to Andrea for her small but crucial contributions in scientific matters.

Dedicated to my grandmother Albine for inadvertently putting me on the path of science.

Table of content

Zusammenfassung

Durch Analyse von microRNA-Expressionsmustern in blutbildendem Gewebe konnten mehrere für die Hämatopoese sowie die Funktion des Immunsystems wichtige microRNAs identifiziert werden. MicroRNA-181a (miR-181a) gehört zu diesen Kandidatengenen, und es konnte bereits gezeigt werden, dass sie durch Modulation der T-Zell-Rezeptor-Aktivität eine kritische Rolle in der Differenzierung und Reifung von T-Zellen spielt. Des Weiteren konnte bei systemischer Inflammation im Mausmodell eine Runterregulierung der miR-181a-Expression in Lymphozyten beobachtet werden. Diese Ergebnisse implizieren eine wichtige Funktion für miR-181a in der Immunhomöostase, vor allem in der Steuerung der inflammatorischen Antwort auf Pathogene.

In Bezug auf diese vorherigen Ergebnisse wollen wir die Rolle von miR-181a in humanen Lymphozyten und speziell in humanen dentritischen Zellen, den primären antigenpräsentierenden Zellen des Immunsystems, aufklären. Wir beabsichtigen dabei, mit einer anti-miR181a-shRNA via lentiviraler Transfektion die Expression von miR-181a in hämatopoetischen CD34-positiven Stammzellen aus humanem Nabelschnurblut stabil zu unterdrücken. Die dabei gewonnenen Stammzellen sollen zu dendritischen Zellen differenziert werden, um die Effekte des Verlusts der miR-181a-Expression sowohl auf die Differenzierung der Zellen als auch auf die Maturation nach mikrobieller Stimulation zu untersuchen. Vorläufige Ergebnisse deuten bereits darauf hin, dass der Verlust von miR-181a in dendritischen Zellen eine Erhöhung der co-stimulatorischen Oberflächenmarker, gesteigerte Zytokinproduktion sowie eine höhere Sensitivität der Zellen gegenüber bakteriellem Lipopolysaccharid nach sich zieht.

Wir beabsichtigen daher, durch Analyse des mit dem Verlust von miR-181a einhergehenden Phänotyps betreffend co-stimulatorischer Marker, Zytokinproduktion und Zellmigration sowie durch die Etablierung einer Liste immunrelevanter Zielgene für miR-181a die Mechanismen aufzuklären, welche es miR-181a erlauben, die Homöostase der Immunantwort auf der initialen Stufe der Antigenerkennung- und präsentation durch dendritische Zellen zu regulieren.

Abstract

Analysis of hematopoietic tissue microRNA expression patterns has identified several microRNAs crucial in hematopoiesis and immune response. Among these, microRNA-181a (miR-181a) has been shown to play a pivotal role in immune cell differentiation and maturation, modulating the sensitivity of T cells against antigens both during differentiation as well as in their mature state. Additionally, downregulation of miR-181a expression in lymphocytes observed during systemic inflammation in mice implicates that miR-181a might be a crucial regulator in the homeostatic response to inflammatory stimuli.

Therefore, we intend to examine the effects of miR-181a on human lymphocytes, focusing our attention on dendritic cells, one of the main antigen-presenting cells (APC) of the immune system. Utilizing an HIV-1 derived lentiviral delivery vector, we will perform a knockdown of miR-181a in human CD34+ hematopoietic stem cell-derived DCs by miR-181a antisense construct shRNA, subsequently studying the effect of miR-181a loss on DC differentiation and maturation in response to microbial stimulus. Preliminary analysis of these miR-181a knockdown DCs shows phenotypic differences like increased co-stimulatory surface markers and cytokine secretion besides a higher sensitivity to bacterial lipopolysaccharide stimulation.

By examining the phenotypic changes in regards to surface marker expression, cytokine production and cell migration produced upon miR-181a knockdown and by establishing a list of immune-relevant target genes for our microRNA of interest we thus aim to elucidate the mechanisms by which miR-181a may govern immune homeostasis on the initial level of antigen recognition and presentation by dendritic cells.

1. Introduction

1.1. Dendritic cells - roles and functions

Since having first been described by Ralph Steinman and Zanvil Cohn in 1973 [1] dendritic cells (DCs) have become the topic of a broad and diverse field of research. Originally defined by their irregular morphology and characteristic branched cytoplasmic projections, the dendrites, dendritic cells have eventually been shown to be composed of a family of various cell types with one common role as "professional" antigen presenting cells (APC), a role defined by the efficient uptake, processing and presentation of antigen to T cells, eliciting activation of the adaptive immune system against said antigen. Hence, dendritic cells form a cornerstone of the adaptive immune response against pathogens.

1.1.1. Hematopoietic origins of dendritic cells

Dendritic cells are a heterogeneous family of cell types of phenotypic and functional diversity [2] which may be broadly categorized into two major subsets: monocyte-derived DCs (moDCs) recruited from the blood in response to acute inflammatory stimuli as well as continuously replenished steady-state DCs acting as sentinels against pathogens [3, 4], with the latter encompassing classical DCs (cDCs) and type I interferon-producing plasmacytoid DCs (pDCs).

All blood cells trace their ancestry back to a pool of self-renewing long-term hematopoietic stem cells (LT-HSCs) in the bone marrow. These cells continuously spawn short-term hematopoietic stem cells (ST-HSCs) which further commit towards multipotent progenitors (MPPs), forfeiting their potential for self-renewal. These intermediate progenitors are classically divided into common myeloid and common lymphoid progenitors (CMPs and CLPs, respectively).

Fig.1. Hematopoietic lineage of dendritic cells

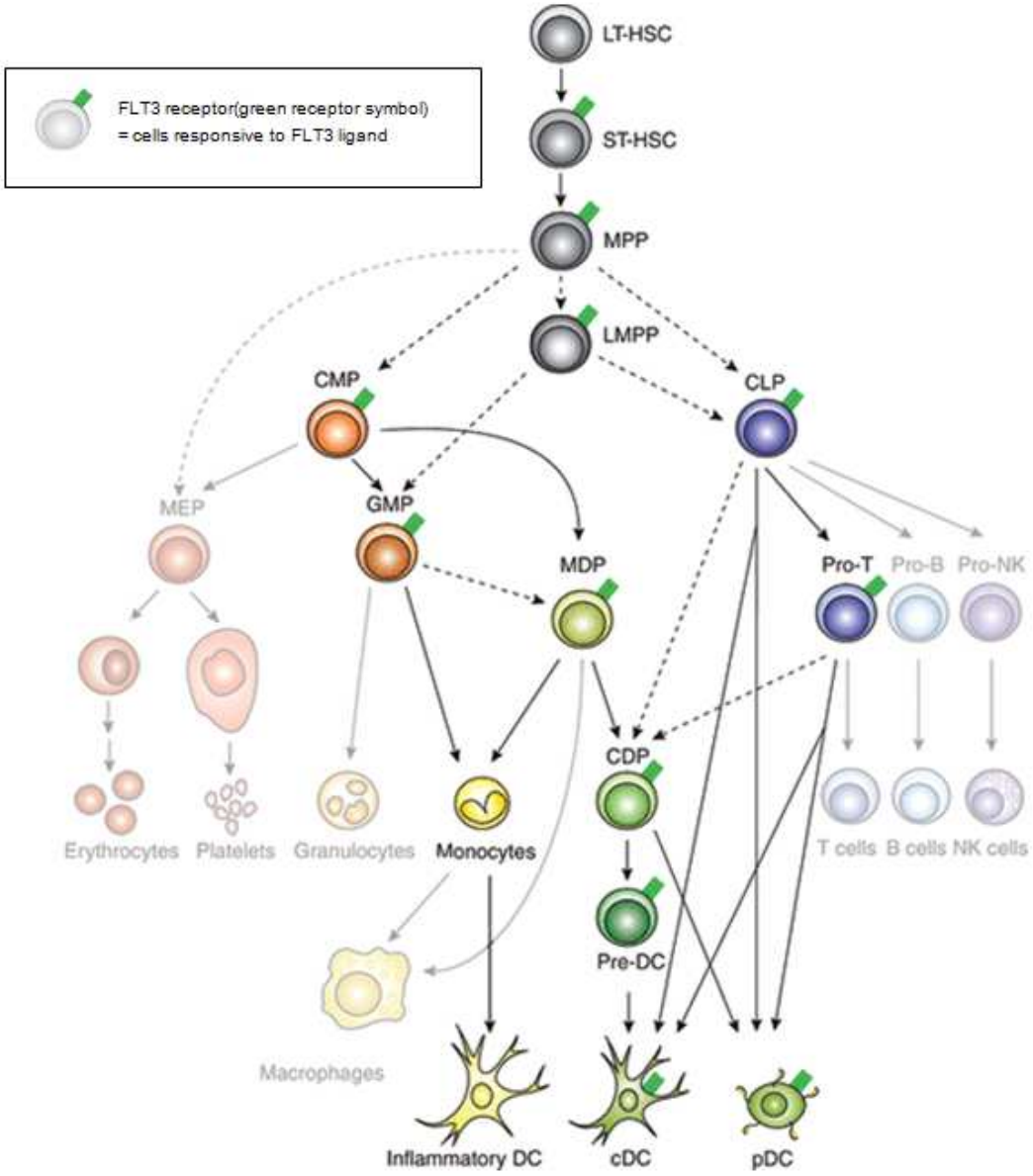

The lineage differentiation flow chart for DCs is depicted; lineages of other hematopoietic cell types branching off are shown in opaque. Dendritic cell lineage commitment is primarily driven by signaling through the Fms-like tyrosine kinase 3 (FLT3) receptor, shown here as a green receptor symbol on the corresponding cells. Short-term hematopoietic stem cells (ST-HSC) derived from their long-term progenitors (LT-HSC) commit towards multipotent progenitors (MPP), then branching off into common progenitors of myeloid (CMP) or lymphoid (CLP) lineage; alternatively, lymphoid-primed progenitors (LMPP) lacking erythrocyte potential may differentiate towards both branches. The myeloid compartment gives rise to granulocyte macrophage progenitors (GMP) and macrophage dendritic progenitors (MDP) which lead into the monocyte / inflammatory DC axis or to the common DC progenitor (CDP) with the potential to differentiate into classical DCs (cDC) or plasmacytoid DCs (pDC). In parallel, lymphoid progenitors are able to turn into cDCs and pDCs either directly or over the generation of CDPs. Alternatively, Pro-T cells from the lymphoid lineage retain the potential to differentiate into cDC and pDC cell populations. (Graphic derived from Schmid, M.A., et al., *Instructive cytokine signals in dendritic cell lineage commitment.* Immunological Reviews, 2010.**234**(1): p. 36.)

DCs may arise from both primitive myeloid-committed as well as lymphoid-committed progenitors. The maintenance of dendritic cell potential throughout the branching and progressively restrictive steps of hematopoiesis is facilitated mainly by signaling through the cytokine receptor Fms-like tyrosine kinase 3 (FLT3, also known as CD135); its binding partner FLT3 ligand was shown to be an indispensable factor for DC development [5-7]. A continuous surface expression of FLT3 signifies the complex lineage of the steady-state DC subsets [8].The recent model of DC development proposes FLT3 expressing subpopulations of both CMPs and CLPs keep an inherent potential to differentiate into DCs [Fig. 1].

1.1.2. Role of dendritic cells in the immune system

Dendritic cells, in their function as professional antigen-presenting cells, facilitate the crucial first steps in initiating the adaptive immune response against a pathogen. Resident in virtually every tissue DCs act as sentinels of the immune system, waiting for a stimulus (e.g. pathogens, excessive cell death or endogenous inflammatory signals) to trigger their inherent activation program which is characterized by three distinct steps: the efficient uptake and processing of antigen in their vicinity followed by their chemotactic migration towards the nearest lymph node where, ultimately, they present the processed antigen to naïve T cells accompanied by instructive costimulatory signals [9].

In their capacity to prime naïve T cells, DCs are unparalleled and they are indispensable in mounting an efficient adaptive immune response. Processed antigenic peptide fragments are loaded onto major histocompatibility complex (MHC) molecules. Naïve T cells may recognize these peptide-MHC-complexes with their T cell receptor (TCR); if the antigenic epitope displayed on the MHC fits the respective TCR the T cell is activated in conjunction with the costimulatory signals produced by the DC [10]. This specific scheme of antigen recognition comprises the linchpin of the adaptive immune response.

However, DCs are not limited to immune activation. They also contribute considerably to immunological tolerance. DCs constantly sample their surroundings, absorbing endogenous antigen in the process. Lacking activating stimulus the DCs digest these self-antigens and present them in a tolerogenic context. In this role DCs may induce apoptosis in self-reactive T cells and promote the generation of immunosuppressive regulatory T cells (T_{Reg} cells) [11, 12].

1.1.3. Maturation of dendritic cells in reaction to stimuli

The program dendritic cells undergo upon encountering a stimulus is termed “maturation”; a DC which has not yet received an activating stimulus is therefore considered an immature DC (iDC) [9]. iDCs are phagocytically active and continually take up and process antigen from their immediate surroundings. However, in their immature state DCs are restricted in their ability to display peptide-MHC-complexes on their cell surface.

Maturation stimuli are received by recognizing pathogen-associated molecular patterns (PAMPs) [13] or endogenous “danger signals” released by cell stress and abnormal cell death [14]. DCs perceive these signals through a plethora of pattern recognition receptors (PRRs) located on the cell surface as well as inside endosomes and the cytosol [15], with the Toll-like receptor (TLR) family being the most prominent group of PRRs. In particular, TLRs recognize components of pathogens as bacterial lipopolysaccharide (LPS) or peptidoglycan, fungal zymosan or viral double-stranded RNA, to name a few [16]. In their conserved specificity for certain ligands TLRs and other PRR families are considered part of the innate immune system.

Upon activation, DCs transiently increase their phagocytosis to ingest as much ambient antigen samples as possible [17]. Roughly four hours after stimulation, phagocytosis is halted and the DCs achieve increased migratory capability by upregulating surface expression of the chemokine receptor CCR7 [18, 19]. Following a gradient of the chemokine receptor ligands CCL19 and

CCL21 the DCs home for adjacent lymphatic vessels, eventually reaching the nearest draining lymph node. In parallel, expression of costimulatory surface molecules and cytokines increases and peptide-MHC complexes commence to be stably presented on the surface of the DC [20, 21]. Having arrived at the lymph node, the DCs may then, influenced by their antigen payload and costimulatory marker pattern, specifically stimulate responses from members of the adaptive immune compartment.

1.2. micro-RNAs - key regulators of gene expression

MicroRNAs (miRNAs or miRs), small non-coding RNAs of approximately 22 nucleotides in length, have progressively emerged as key regulators of genes in plants and animals since the discovery of the microRNA lin-4 in the popular model organism *Caenorhabditis elegans* [22, 23]. As their cousins, the small interfering RNAs (siRNAs) [24], microRNAs act through a process called RNA interference (RNAi) [25]. Here, in conjunction with several proteins, pre-processed microRNA molecules target complementary sequence stretches in mRNAs, promoting their degradation. A single microRNA may exert its function over many mRNA transcripts, provided these transcripts contain one or several complementary sites. Therefore, microRNAs are able to influence gene expression levels in often very complex ways.

1.2.1. Origins and mechanisms

Phylogenetic analysis has shown that RNAi is an ancestral mechanism, probably already existent in the most recent common ancestor of all eukaryotes; notwithstanding that some eukaryotic organisms appear to have later lost their RNAi machinery [26]. It is suggested that the evolutionary origin of RNAi lies in a defense mechanism against RNA viruses and transposons, a function which RNAi fulfills in plants until this very day [27]. Here, viral or transposon-derived double-stranded RNAs are recognized and cut by

proteins, and the resulting small RNA fragments are used to suppress translation and initiate degradation of RNAs with homologous sequence.

By providing this machinery with endogenous double-stranded RNA transcripts eukaryotic organisms have repurposed this erstwhile defense mechanism against foreign RNA into a tool fortuning their own gene expression. In RNAi, a primary RNA transcript, the pri-miR, is processed by the nuclear RNAse Drosha into a 70-nucleotide double-stranded stem-loop precursor miR (pre-miR) which is subsequently cut into 20-25 nucleotides long double-stranded microRNA fragments by the endonuclease Dicer and incorporated into the multi-protein RNA-induced silencing complex (RISC) [28-30]. Ultimately, RISC facilitates translational silencing by binding to and cleaving mRNAs with sequences complementary to its incorporated microRNA [28]. An alternative pathway depending on the so-called RITS complex is even able to silence genes on a transcriptional level by binding to a nascent mRNA chain while initiating the spread of heterochromatin [31]. Thus, what may once have begun as a defense mechanism infections against rogue RNA elements has evolved into a staple mechanism of eukaryotic gene regulation [32].

1.2.2. micro-RNAs in the immune system

A plethora of microRNAs were initially identified by classical cloning techniques and later by genomic sequence analysis for conserved stem-loop structures [33-35]. In humans, 1000 unique microRNAs were predicted [36], possibly exerting control over more than 60 % of the human genes [37]. Besides their effect on biological processes like development, tissue growth and metabolism [38], microRNAs appear to play a crucial role in the adjustment and fine tuning of the immune system, both on the level of hematopoietic differentiation [39-41] as well as in the modulation of the immune response itself [41, 42].

1.3. miR-181a

One microRNA discovered through analysis of hematopoietic tissue microRNA expression patterns is miR-181a [39]. First described as a contributing factor in megakaryoblast differentiation [43] and as a potential marker for acute myeloid leukemia and primary glioblastoma [44, 45], miR-181a was soon established to participate in the maturation process of T cells, modulating their sensitivity against antigens both during differentiation as well as in their mature state [46].

1.3.1. Established functions of miR-181a in the immune system

Recognizing the pivotal regulatory role of miR-181a in the selection of T cell progenitors in the thymus, further studies into the matter were conducted, demonstrating that miR-181a directly tunes the T cell receptor (TCR) activation threshold of naive CD4+CD8+ double positive thymocytes [47]. Utilizing an shRNA [48] to knock down miR-181a, it was validated that decreased miR-181a levels in double positive thymocytes prevented the negative thymic selection of T cells with a strong reaction towards self-antigens.

Nevertheless, the influence of miR-181a on immune cells is not confined to restricting T cell autoreactivity; as of late, it has been implicated in transplant alloreactivity [49], natural killer T cell development [50-52] and as a potential biomarker for metabolic syndrome and coronary artery disease risk in obese patients [53]. The latter article correlated decreased miR-181a expression with an increased systemic inflammatory responsiveness.

These implications could be consecutively reinforced by other studies, hinting that miR-181a levels increase as a homeostatic response to inflammatory stimuli by exerting an anti-inflammatory effect in monocytes and macrophages [54-56]. In mice, miR-181a blood concentrations increased twofold two hours after transient inflammatory challenge with bacterial

lipopolysaccharide (LPS). Comparably, miR-181a increase could be observed in macrophages isolated from LPS-challenged mice. Concurrently, miR-181a baseline levels were significantly elevated in a diabetic mouse model due to their chronic low-grade inflammation; this effect could be counteracted by administering anti-diabetic drugs to the mice [56].

In addition, Langerhans cells (LCs), an epidermal DC subset, were found to express considerable levels of miR-181a in comparison to dermal DCs [57]. Since LCs are constantly confronted with bacterial signals from the commensal skin flora they are required to maintain a tolerogenic phenotype to eschew triggering skin inflammation [58, 59]. This may give a further hint to miR-181a being involved in the regulation of the immunogenicity versus tolerogenicity axis in DCs.

1.3.2. Potential functions in dendritic cell development and maturation

Experiments in cell culture corroborated the anti-inflammatory effect of miR-181a, with overexpression of the microRNA dampening inflammation signaling in THP-1 monocyte cell line by targeting key inflammatory signaling pathway factors such as IL1a, IL6 and TNF-α; in reverse, an increase of inflammatory signaling was observed in cells knocked down for miR-181a [55].

An analogous study on the impact of miR-181a in ox-LDL-stimulated dendritic cells emphasized these findings. A distinct effect of miR-181a on pro-inflammatory signals as well as on the expression of CD83, CD40 and CD80/86, surface markers indicative for DC maturation, was observable [54].

2. Rational of this thesis

Together, the result presented above suggest a central role for miR-181a as an anti-inflammatory feedback system in cells of the immune system, and in dendritic cells in particular. As was shown in mice [56], chronic inflammation causes an increase in miR-181a expression in DCs isolated from lymph nodes, implicating that miR-181a acts as a failsafe mechanism against overshooting immune reactions and improper activation of "bystander" immature dendritic cells in an inflammatory setting. In turn, a decrease of steady-state miR-181a levels may alleviate the brake this particular microRNA may exert on the inflammatory response and maturation of dendritic cells.

It is thus expected that an shRNA-mediated knock-down of miR-181a during the differentiation of hematopoietic progenitor-derived dendritic cells will result in a population of immature DCs more susceptible to inflammatory triggers or a generally more mature phenotype prior to stimulation. Preliminary results from miR-181a knock-down DCs implicate increased DC maturity and a lower activation threshold on challenging the cells with pathogen-associated molecular patterns like LPS. Further, miR-181a knock-down DCs are assumed to react more drastically in response to proinflammatory signals, resulting in more vigorous upregulation of costimulatory surface markers, increased cytokine secretion and possibly higher chemotactic motility towards lymphatic chemokines.

3. Materials and methods

3.1. Buffers and solutions

The compositions of the buffers and solutions used in this work are listed below in Table 1.

Table 1. Buffers and solutions

buffer / solution	composition
10x PBS stock	1.37 M NaCl, 27 mM KCl, 43 mM Na_2HPO_4, 14 mM KH_2PO_4, pH 7.3
PBST	0.05 % Tween-20 in 1x PBS
10x SDS buffer	30 g/l Tris, 144 g/l glycine, 10 g/l SDS
blocking solution	5 % non-fat dry milk in PBST
blotting buffer	25 mM Tris/HCl, 192 mM glycine, 20 % methanol
Ponceau S solution	1 g/l Ponceau S, 5 % acetic acid
2x HBS buffer	16 g/l NaCl, 13 g/l HEPES, 105 mg/l Na_2HPO_4, pH 7.0
MACS buffer	5 mM EDTA, 0.5 % BSA in 1x PBS
ACK buffer	150 mM NH_4Cl, 1 M $KHCO_3$, 0.1 mM EDTA, pH 7.3
FACS buffer	1 % BSA, 0.02 % Na_3N in 1x PBS
LB medium	10 g/l tryptone, 5 g/l yeast extract, 10 g/l NaCl, pH7.0
5x KCM buffer	0.5 M KCl, 0.15 M $CaCl_2$, 0.25 M $MgCl_2$

3.2. Cytokines

All cytokines used in this study were supplied by Peprotech, Vienna, Austria.

3.3. Plasmids

For lentivirus production the 2nd generation packaging plasmid W262 (psPAX-2) [Fig 2.B] and the VSV-G envelope plasmid W263 (pMD2.G) [Fig 2.A] were used in conjunction with an anti-miR-181a shRNA pmiRZip-181a lentivector (based on pGreenPur™) or an empty control miRZip-000 lentivector (based on pGreenPur™) [Fig 2.C].

Fig.2. Plasmids

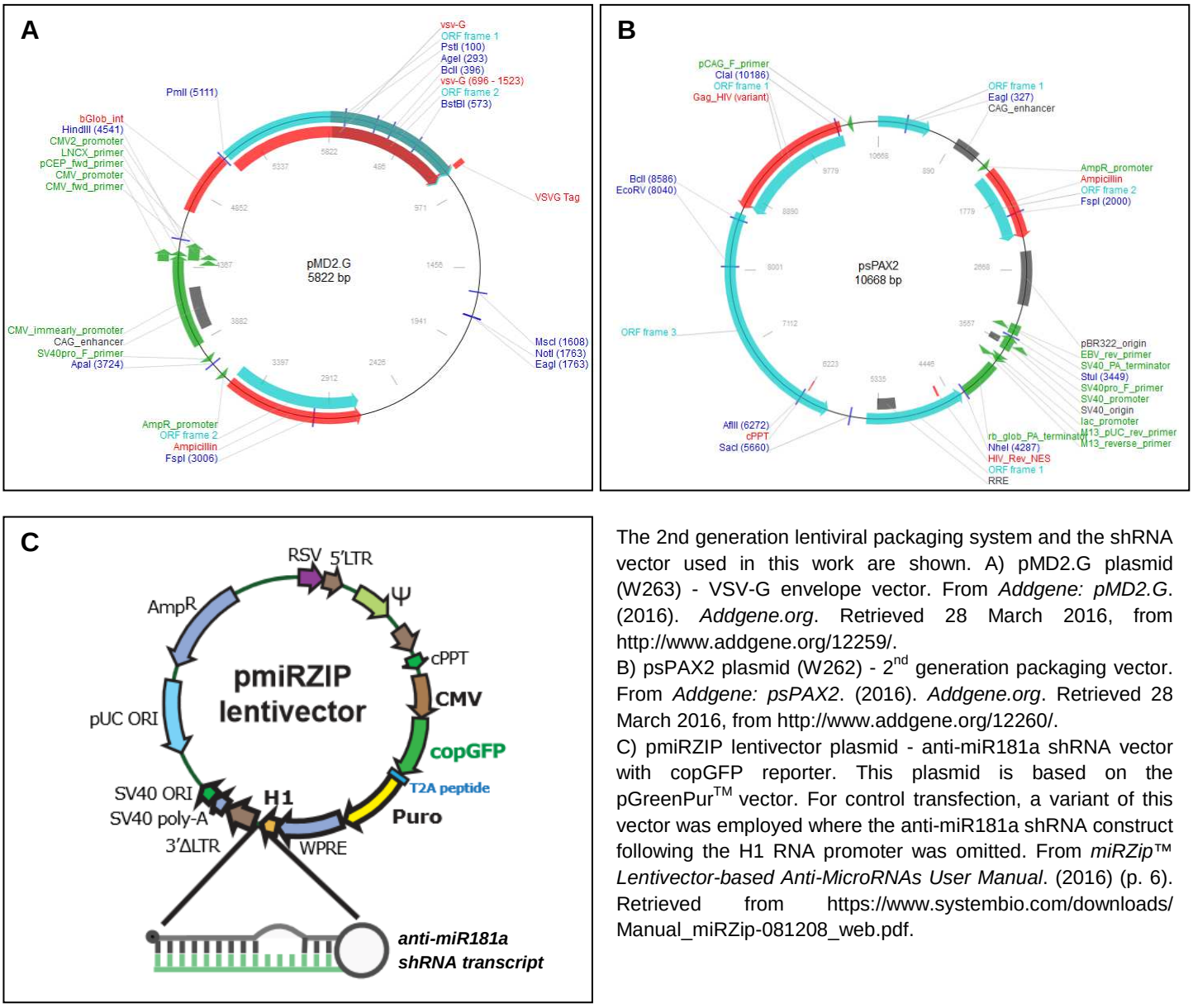

The 2nd generation lentiviral packaging system and the shRNA vector used in this work are shown. A) pMD2.G plasmid (W263) - VSV-G envelope vector. From *Addgene: pMD2.G*. (2016). *Addgene.org*. Retrieved 28 March 2016, from http://www.addgene.org/12259/.
B) psPAX2 plasmid (W262) - 2nd generation packaging vector. From *Addgene: psPAX2*. (2016). *Addgene.org*. Retrieved 28 March 2016, from http://www.addgene.org/12260/.
C) pmiRZIP lentivector plasmid - anti-miR181a shRNA vector with copGFP reporter. This plasmid is based on the pGreenPur™ vector. For control transfection, a variant of this vector was employed where the anti-miR181a shRNA construct following the H1 RNA promoter was omitted. From *miRZip™ Lentivector-based Anti-MicroRNAs User Manual*. (2016) (p. 6). Retrieved from https://www.systembio.com/downloads/Manual_miRZip-081208_web.pdf.

3.4. Cell culture

All mammalian cells were incubated at 37 °C at 5 % CO_2. Unless noted otherwise, centrifugation of cells was performed at 1200 rpm for 5 min.

3.4.1. HEK293T cells

HEK293T cells maintained in DMEM plus 10% FCS, 2.5 mM L-glutamine, 125 U/ml penicillin and 125 U/ml streptomycin. HEK293T cells were grown in 10cm NUNC plates and split every 48 h. Cell splitting was performed by sucking off the medium, adding 2 ml of trypsin solution to the plates followed by the addition of 10 ml fresh DMEM. Cells were fully detached by gently tapping the plate. The cell suspension was subsequently centrifuged and the supernatant was removed. Cells were seeded in 10cm plates in 10 ml of DMEM medium.

3.4.2. Human cord blood CD34+ stem cells

CD34+ hematopoietic stem cells were isolated from human cord blood and initially seeded for expansion in Nunclon Delta 24 well cell culture plates (Thermo Scientific, Vienna, Austria) at 10^6 cells per well for one to three days in X-vivo 15 medium (Biowhittaker, Walkersville, MD, USA) plus 2.5 mM GlutaMAX, 125 U/ml penicillin and 125 U/ml streptomycin. To trigger expansion of the cells the cytokines Flt3L, SCF and TPO were added at 50 ng/ml each. During lentiviral transfection the medium was changed to CellGro plus 10% FCS, 2.5 mM GlutaMAX, 125 U/ml penicillin and 125 U/ml streptomycin with GM-CSF (100 ng/ml), Flt3L (50 ng/ml), SCF (20 ng/ml) and TNF-α (2.5 ng/ml). After five days and subsequent flow cytometric sorting for transfected cells the cells were set up in Nunclon Delta 24 well cell culture plates (Thermo Scientific, Vienna, Austria) at 10^5 cells per well in RPMI-1640 medium plus 10% FCS, 2.5 mM GlutaMAX, 125 U/ml penicillin and 125 U/ml

streptomycin under addition of GM-CSF (100 ng/ml) and IL-4 (25 ng/ml), stimulating their differentiation into dendritic cells.

3.4.3. Human peripheral blood CD14+ monocytes

CD14+ monocytes were isolated from human peripheral blood and set up in Nunclon Delta 24 well cell culture plates (Thermo Scientific, Vienna, Austria) at 10^6 cells per well in RPMI-1640 medium plus 10% FCS, 2.5 mM GlutaMAX, 125 U/ml penicillin and 125 U/ml streptomycin with the addition of GM-CSF (100 ng/ml). The cells were incubated overnight in order for them to recuperate from the isolation procedure. Subsequently, the cells were kept in this mix for lentiviral transfection and IL-4 (50 ng/ml) was added immediately or up to 72 h after the start of the transfection according to the experimental plan. The cells were centrifuged, washed and replated in Nunclon Delta 24 well cell culture plates (Thermo Scientific, Vienna, Austria) at 10^6cells per well after the retroviral transfection and differentiated into dendritic cells in RPMI-1640 medium with GM-CSF (100 ng/ml) and IL-4 (50 ng/ml) for five days onwards from the initial IL-4 dose.

3.5. Isolation of human cord blood CD34+ stem cells

Cord blood was collected from healthy donors after caesarean section or full-term delivery. Cord blood samples were diluted 1:1 in PBS and a density gradient centrifugation over Lymphoprep (Axis-Shield PoC AS, Oslo, Norway) was performed. The diluted cord blood (max. 25 ml per tube) was layered over 20 ml of Lymphoprep in a 50 ml conical bottom tube. The tubes were centrifuged for 30 min at 1400 rpm with brakes disabled. After centrifugation the mononuclear fraction containing the CD34+ cells was discernable as a white ring over the Lymphoprep phase. The cell-containing phase was carefully collected and transferred to a fresh 50 ml tube (max. 20 ml per tube). The tubes were filled to 50 ml with PBS and centrifuged at 1600 rpm for 8 min. After removal of the supernatant the cell pellet was resuspended in a total of

5 ml of ACK erythrocyte lysis buffer and the tubes were incubated on ice for 10 min after which lysis was stopped by adding 45 ml of PBS. The tubes were centrifuged for 20 min at 700 rpm and the cells were resuspended in 1 ml MACS buffer. Cell count was determined. The cells were washed with PBS and resuspended in 80 µl MACS buffer per 10^7 cells. EasySep Human CD34 Positive Selection Kit (Stemcell Technologies, Grenobles, France) was used to select for the CD34+ fraction. All further steps were performed according to the kit's protocol. The cell count of the purified fraction was determined and the cells were seeded for expansion as described in paragraph 3.4.2.

3.6. Isolation of human peripheral blood CD14+ monocytes

Peripheral blood was collected from healthy donors and diluted 1:1 in PBS. A density gradient centrifugation over Lymphoprep (Axis-Shield PoC AS, Oslo, Norway) was performed. The diluted blood (max. 25 ml per tube) was layered over 20 ml of Lymphoprep in a 50 ml conical bottom tube. The tubes were centrifuged for 30 min at 1400 rpm with brakes disabled. After centrifugation the mononuclear fraction containing the CD14+ monocytes was discernable as a white ring over the Lymphoprep phase. The cell-containing phase was carefully collected and transferred to a fresh 50 ml tube (max. 20 ml per tube). The tubes were filled up to 50 ml with PBS and centrifuged at 1600 rpm for 8 min. After removal of the supernatant the cell pellet was resuspended in 1 ml MACS buffer. Cell count was determined. The cells were washed with PBS and resuspended in 80 µl MACS buffer per 10^7cells. A MACS LS cell separation column (Miltenyi Biotec, Bergisch Gladbach, Germany) was used for positive selection of CD14+ monocytes. 20 µl of CD14 MicroBeads (Miltenyi Biotec, Bergisch Gladbach, Germany) were added to the cells and the mix was incubated for 15 min at 4 °C. Meanwhile, the column was placed in the magnetic field and equilibrated with 3 ml of MACS buffer. The cell suspension was applied to the column and washed three times with 3 ml of MACS buffer. Afterwards, the column was removed from the magnetic field, placed on a fresh 15 ml V bottom tube and the cells were flushed out with 5 ml of MACS buffer using a plunger. The positively selected CD14+

monocytes were counted, washed with PBS and the cells were seeded as described in paragraph 3.4.3.

3.7. Transfection of HEK293T cells and packaging of lentiviral vector

HEK293T cells were used as packaging cells for our lentiviral vectors. The day before the transfection an approximately 90 % confluent 10cm dish of HEK293T cells was split (see paragraph 3.4.1.) and reseeded 1:8 in 3 ml of medium into 6cm cell culture dishes which were grown overnight up to a confluency between 50 to 70 %, as assessed by microscopy. The transfection mix was prepared in 15 ml V bottom tubes. The packaging plasmids W262 and W263 were added at 3 µg each together with 1 µg of the shRNA or control vector plasmid. The DNA was mixed with 63 µl CaCl2 solution and 430 µl of sterile ddH2O were added. Then, the tubes were placed on a vortex mixer at full speed and 1 ml of 2xHBS buffer was applied dropwise into the vortex. The transfection mix was quickly spun down at 1000 rpm. Meanwhile, 3 µl of chloroquine solution were added to each 6cm dish. The dishes were incubated for 5 min and 1 ml of the transfection mix was carefully dripped onto each plate. After 6 h of incubation the medium on the dishes was changed for 3 ml of fresh DMEM plus 10% FCS, 2.5 mM L-glutamine, 125 U/ml penicillin and 125 U/ml streptomycin. The dishes were allowed to incubate for 48 h and, subsequently, the supernatant containing the lentiviral particles for the first infection round was collected with a syringe and filtered through a 0.22 micron syringe filter. The cell dishes were again covered with 2 ml of fresh medium and incubated for another 24 h after which the supernatant for the second infection round was collected and filtered.

3.8. Lentiviral transduction of human cord blood CD34+ stem cells

Lentiviral transduction was performed using Retronectin (Takara Bio Europe/Clontech, Saint-Germain-en-Laye, France), a recombinant protein facilitating binding between the lentiviral particles and the target cells. A

CellStar 24 well suspension culture plate was coated with Retronectin by adding 250 µl of Retronectin solution per well followed by incubation at 37 °C for 3 h. Afterwards, the Retronectin solution was taken off the plate and collected; a batch of Retronectin solution could be used for coating up to three times. 500 µl of DMEM plus 10% FCS was applied to each well for 15 min in the incubator. The DMEM was sucked off and 500 µl of viral supernatant (see paragraph 2.3.6.) was added per well. The lentiviral particles were allowed to bind to the Retronectin for 3 h at 37 °C in the incubator. CD34+ stem cells were added to the plates at 2-5 x 10^5 cells per well under the addition of 500 µl of CellGro medium plus 10% FCS, 2.5 mM GlutaMAX, 125 U/ml penicillin and 125 U/ml streptomycin. The cells were supplemented with the cytokines GM-CSF (100 ng/ml), Flt3L (50 ng/ml), SCF (20 ng/ml) and TNF-α (2.5 ng/ml). The next day, another 250 µl of viral supernatant were added to each well and the cells were allowed to proliferate for another 4 days and collected for sorting.

3.9. Lentiviral transduction of human peripheral blood CD14+ monocytes

Retronectin-coated plates were prepared as described in paragraph 2.3.7. Since standard lentiviral transduction of CD14+ monocytes yields very low amounts of transduced cells the protocol required the addition of non-replicating SIV-based viral helper particle which was produced with the same method as the lentiviral vector particles (see paragraph 3.8.). For the transduction of CD14+ monocytes 250 µl of SIV helper viral supernatant were added to the Retronectin-coated wells in addition to the 500 µl of vector viral supernatant. The plates were incubated for 3 h at 37°C to allow binding of the viral particles and 10^6 cells in 500 µl RPMI-1640 medium plus 10% FCS, 2.5 mM GlutaMAX, 125 U/ml penicilin,125 U/ml streptomycin were added per well. The cells were supplemented with GM-CSF (100 ng/ml). IL-4 (50 ng/ml).

3.10. Cell sorting

Transduced cells were sorted by flow cytometry with GFP as positive selection marker. After transduction, the medium containing the cells was taken off the plates and collected. The plates were washed with 500 µl of PBS per well which was added to the collected medium. The cells were spun down and the supernatant was removed. The pellet was resuspended in 300 µl of PBS plus 2 % FCS and sorted for GFP positives. The sorted fraction was resuspended in medium and seeded as described in paragraph 3.4.2.

3.11. Cell freezing and thawing

For freezing, cells were harvested, centrifuged at 1200 rpm for 5 min, transferred into 1 ml of FCS plus 10 % DMSO and filled into Nunc Cryotubes (Thermo Scientific, Vienna, Austria). Cryotubes were slowly cooled down to -80 °C in a Nalgene Cryocontainer filled with 2-propanol over the course of two days and kept further in the -80 °C freezer. CD34+ cells were frozen at 10^6 cells per ml. For HEK293T a 90 % confluent 10cm dish was harvested and split into two Cryotubes . For thawing, frozen cell aliquots were quickly thawed by swirling them in a 37 °C water bath until the content of the tube was liquid. The cells were then washed with 10 ml of DMEM plus 10 % FCS per 1 ml aliquot and spun down at 800 rpm for 3 min. Supernatant was removed and the cells were resuspended in the corresponding culture medium.

3.12. 3D collagen matrix cell migration assay

Dendritic cells matured with LPS were harvested with the differentiation medium and transported on ice to the facility where the assays were performed; transport on ice took approximately 30 min. At the facility the cells were allowed to recuperate for 30 min at 37 °C in the incubator. Meanwhile, the chambers for the assay were prepared. For the assay a 6cm cell culture dish with a 1 cm diameter hole cut into the bottom is required. A cover slip was

used to seal the hole by gluing it onto the bottom of the plate with paraffin wax. Then, another cover slip was put over the hole from the inside of the dish and glued on with paraffin wax, leaving open a small opening (about one fifth of the hole's area not being covered), thus creating the migration assay chamber [Fig. 3].

Fig.3. 3D collagen matrix gel chamber assembly

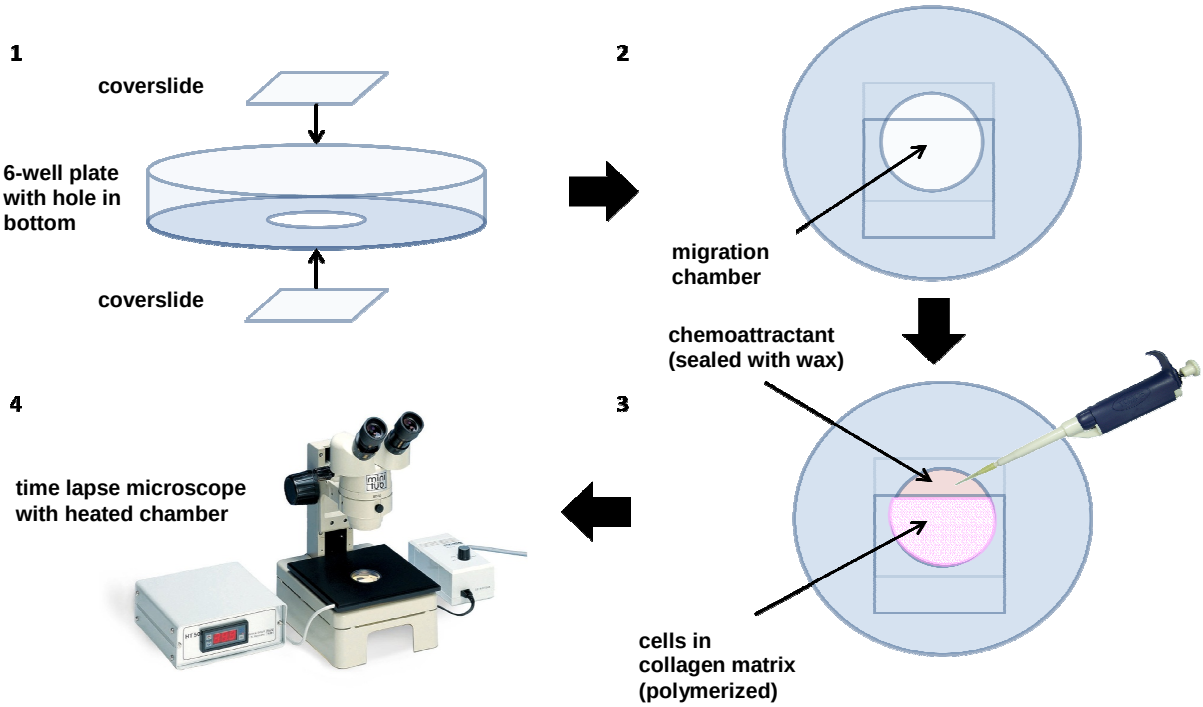

Schematic representation demonstrating the assembly of the chambers used in the 3D collagen matrix assay.1) Assembly of the migration chamber, cover slides are fixed to the 6-well plate with paraffin wax 2) Schematic of the assembled migration chamber 3) Cells in collagen mix are added and the collagen is allowed to polymerize for 30 min at 37 °C. Afterwards, chemoattractant diluted in RPMI medium is added to the opening on top of the chamber, which is sealed with a layer of paraffin wax. The chemoattractant quickly diffuses into the collagen gel, creating a gradient. 4) Cell migration is analyzed on a heated time-lapse microscope.

Consecutively, the cells were spun down and resuspended in 100 ml of RPMI medium with 10 % FCS at 100 000 cells per 100 ml. The collagen gel was prepared by mixing 15 µl of 10M NaHCO3 with 30 µl of 10x MEM followed by the addition of 225 µl of human recombinant collagen solution. 200 µl of the

resulting collagen solution were then carefully mixed with 100 µl of suspended cells and filled into the migration chambers up to the edge of the inner cover slip (approximately 150 µl per chamber). The chambers were placed in the incubator at 37 °C for 40 min with the opening of the chamber facing up, allowing the collagen gel to polymerize. Afterwards, the volume of the opening left out in the chambers was filled with RPMI medium containing 2.5 ng of human CCL19 per ml and the chamber's opening was sealed over with paraffin wax. The human CCL19 diffuses into the collagen gel with the embedded dendritic cells creating a gradient of CCL19 towards the liquid phase. The chambers were placed in 37 °C heated microscopes with 5 % CO_2atmosphere and the migration assay was started. Migration of the dendritic cells in the CCL19 gradient was followed taking a picture every minute for a total of 6-8 hours.

3.13. FACS analysis

10^4-10^5 cells were transferred to a 1 ml Micronic tube and the supernatant was removed after centrifugation at 1400 rpm for 5 min at 4 °C. Centrifugations for washing steps were performed at the same settings. Cells were washed once with 0.5 ml of FACS buffer and resuspended in 40 µl of FACS buffer with the addition of 5 µl of 150 mg/ml Beriglobin human IgG solution (CSL Behring, Vienna, Austria). Cells were gently vortexed and incubated for 30 min at 4 °C. Then, 10 µl of the corresponding fluorochrome- or biotin-conjugated primary antibody dilution mix (for antibody dilutions, see Table 2) were added and the cells were incubated for 30 min at 4 °C. Cells were washed with 0.5 ml of FACS buffer and resuspended in 40 µl of FACS buffer. In case that the primary antibody dilution mix incorporated biotin-conjugated antibody, another incubation step with 10 µl of 1:100 diluted streptavidin-PerCP secondary antibody (BD Biosciences GmbH, Schwechat, Austria) was performed for 30 min at 4 °C, followed by washing with 0.5 ml of FACS buffer and resuspension in 40 µl of FACS buffer. FACS analysis was performed on a BD LSRII cytometer using the BD FACSDiva software

(BD Biosciences GmbH, Schwechat, Austria). Further analysis of the generated data was performed with the FlowJo Single Cell Analysis software.

Table 2. Primary and secondary Western blot antibodies

epitope	supplier	dilution factor	conjugate
CD1a	BioLegend	1:20	Pacific Blue
CD86	BD Biosciences	1:5	PE
CD83	BD Biosciences	1:5	PE
CD80	BD Biosciences	1:5	biotin

3.14. Cell lysis

Cells were harvested, centrifuged and transferred into 25µlper 10^5 cells of lysis buffer supplemented with cOmplete EDTA-free protease inhibitor cocktail tablets (Roche Diagnostics GmbH, Mannheim, Germany). Lysis was achieved by sonication on ice twice for 30 sec, interrupted by a 1 min cooldown period. Lysates were either used directly for further experiments or immediately frozen for storage at -80 °C.

3.15. SDS-PAGE gel

Gels were prepared according to Table 3. Loading dye was added to the cell lysates, which were vortexted, heated at 95 °C for 5 min and spun down for 30 sec at maximum speed. Cell lysates were loaded onto the gel and the gels were run in 1x SDS running buffer at 50 V until the running front had reached the separating gel. Afterwards, the voltage was increased to 100-150 V until completion of the gel run. The gels were dyed for 1 min in Coomassie Brilliant Blue and destained in tap water on the shaker (changing the water several times) until any excess dye was removed and the bands were clearly visible. Destained gels were further used for Western blot.

Table 3.Western blot gel preparation

running gel ... 10%		
H_2O	3,35 ml	5 ml
Tris 1,5M pH 8,8	2,5 ml	3,75 ml
Bis-/acrylamid 29:1	3,5 ml	5,25 ml
SDS 20%	12,5 µl	18,75 µl
TEMED	10 µl	15 µl
APS 10%	100 µl	150 µl
Final volume	**10 ml (2 gels)**	**15 ml (4 gels)**

stacking gel ... 5%		
H_2O	1,67 ml	2,67 ml
Tris 0,5M pH 6,8	2,50 ml	4,00 ml
Bis-/acrylamid 29:1	825 µl	1,32 ml
SDS 20%	8 µl	12,5 µl
TEMED	15 µl	24 µl
APS 10%	50 µl	80 µl
Final volume	**5 ml (2 gels)**	**8 ml (4 gels)**

3.16. Western blot

Blotting sandwiches were assembled in transfer buffer the following order from anode to cathode: a sponge, 2 sheets of filter paper, a polyvinylene difluoride membrane (PVDF; Immobilon-P, Millipore, MA), the SDS-PAGE gel, 2 sheets of filter paper, a sponge; the membrane was soaked in pure methanol for 15 sec beforehand. The transfer was performed at 100 V for 30-60 min at 4 °C. After successful transfer, the blotting sandwich was disassembled and the PVDF membranes were incubated in blocking solution for 3 h on the shaker. Primary antibody solution was prepared by diluting the corresponding primary antibody in 10 ml of blocking solution according to the dilution factor indicated in Table 5. Membranes were incubated in primary antibody solution o/n at 4 °C on the shaker. Afterwards, membranes were carefully rinsed three times with PBST and washed four times in PBST for 10 min on the shaker. Secondary antibody solution was prepared by diluting the corresponding HRP-conjugated secondary antibody in 10 ml of blocking solution according to the dilution factor indicated in Table 4. Membranes were incubated in secondary antibody solution for 1 h at room temperature on the shaker. Membranes were again carefully rinsed three times with PBST and

washed four times in PBST for 10 min on the shaker. SuperSignal West Pico Chemoluminescent Substrate (Pierce Biotechnology) was used for protein detection by chemoluminescence. Blots were developed under a Lumi-Imager (Roche Diagnostics GmbH, Vienna, Austria).

Table 4. Primary and secondary Western blot antibodies

primary antibody	supplier / ref #	dilution factor	isotype
p44/42 (ERK1/2)	CST / # 9102	1: 1000	rabbit
phospho-p44/42 (p-ERK1/2)	CST / # 9101	1 : 1000	rabbit
p38 MAPK	CST / # 9212	1 : 1000	rabbit
phospho-p38 MAPK	CST / # 9211	1 : 1000	rabbit
SAPK/JNK	CST / # 9252	1 : 1000	rabbit
phospho-SAPK/JNK	CST / # 9251	1 : 1000	rabbit
calnexin	CST / # 2433	1 : 1000	rabbit

secondary antibody	supplier	dilution factor	conjugate
ImmunoPure goat anti-rabbit IgG	Pierce Biotechnology	1:5000	HRP

3.17. Transformation of bacterial cells

The E. coli strain DH5α was used in all transformations. Frozen bacterial aliquots were thawed on ice for 10 min and 100 µl of the thawed cells were mixed with 100 µl 1xKCM buffer and 1 ng of plasmid DNA. The cells were gently mixed and incubated 10 min on ice, followed by incubation at room temperature for another 10 min. 500 µl of LB medium were then added and the cells were shaken for 60 min at 37 °C. After spinning down for 1 min at maximum speed, the cells were resuspended in 50 µl of LB medium and streaked on a selective agarose plate containing 50 µg/ml ampicillin . Single cell colonies were obtained 24 h later after incubation at 37 °C.

3.18. Production of plasmids

A single cell colony picked from an agarose plate of bacteria transformed with the corresponding plasmid was set up in a 5 ml LB medium pre-culture containing 50 µg/ml ampicillin for 8 hours at 30 °C on the shaker. Afterwards, 1 ml of the pre-culture was used to inoculate 500 ml of LB medium containing 50 µg/ml ampicillin which was incubated overnight at 30 °C on the shaker. Bacterial cultures were further processed using the QIAGEN Plasmid Maxi Kit (Qiagen N.V., Hilden, Germany) for plasmid purification and all further steps were performed according to the kit's user manual. DNA concentrations were determined using a NanoDrop 2000c spectrophotometer (Thermo Scientific, Vienna, Austria).

3.19. Data analysis

Analysis of the data obtained in this work was performed using the following tools and software.

3.19.1. microRNA target prediction

The tools used for microRNA target prediction were Targetscan (http://targetscan.org/), miRanda (http://www.microrna.org/) and PicTar (pictar.mdc-berlin.de/), using the corresponding preset parameters.

3.19.2. Cell tracking

Analysis of the time-lapse images acquired in the 3D collagen matrix cell migration assay was performed with Fiji. Subtraction of the average intensity z-projection was carried out to exclude stationary artifacts in the pictures. The plugin Trackmate was utilized in tracking the migrating cells employing the Log detector setting for spot detection and the LAP tracker algorithm for computing

the separate tracks. Tracks with duration below ⅔ of the total elapsed time of the assay or a number of distinct spots below ⅓ of the maximum number of spots possible per track were excluded from further analysis. XY coordinates of the tracks were derived and average speed and directionality ratio for each condition were determined in Microsoft Excel with the DiPer macro tool collection [60].

4. Results

The miR-181a knockdown DCs generated for this study present themselves with a number of phenotypic changes. Primarily, an increase in costimulatory surface markers as well as elevated secretion of proinflammatory cytokines upon LPS stimulation could be observed. Analysis of the gene expression patterns of miR-181a knockdown DCs hint at several mechanisms which may be responsible for the measured phenotypic alterations. These will be discussed in the following chapters.

In addition, we were able to successfully transfect PBMCs with our lentiviral miR-181a shRNA vector, using SIV-derived virion-like "helper" particles in order to overcome the natural resistance of PBMCs against lentiviral infection, a method that will also be reviewed below.

4.1. Increased costimulatory surface markers in miR-181a knockdown DCs

As hypothesized, the knockdown of miR-181a in human cord blood-derived CD34+ DCs led to a more activated dendritic cell state. Increased expression of the costimulatory markers CD86 and CD80 was observed upon exposure to bacterial LPS stimuli, albeit to varying magnitude between different donors [Fig 4.]. Additionally, the cell surface levels of both markers were found to be already increased in non-stimulated miR-181a knockdown iDCs as compared to control vector-transfected iDCs, the effect being most pronounced for CD86. An almost twofold increase in CD86 positive cells within the first 9 hours of activation was measured. Interestingly, 24 hours after LPS stimulation a virtually identical level of surface expression was reached for both surface markers. It appears that the knockdown of miR-181a favors spontaneous maturation of DCs and allows for a much more sudden upregulation of the aforementioned costimulatory receptors after stimulation. Possibly, one or several effects of the microRNA knockdown facilitate a poised state in the promoters of the genes coding for these markers, allowing them to reach peak expression at a much earlier stage of the maturation program. This

pre-activation of the costimulatory genes may also encourage spontaneous maturation of the affected iDCs.

Figure 4. Costimulatory surface marker expression in miR-181a knockdown DCs

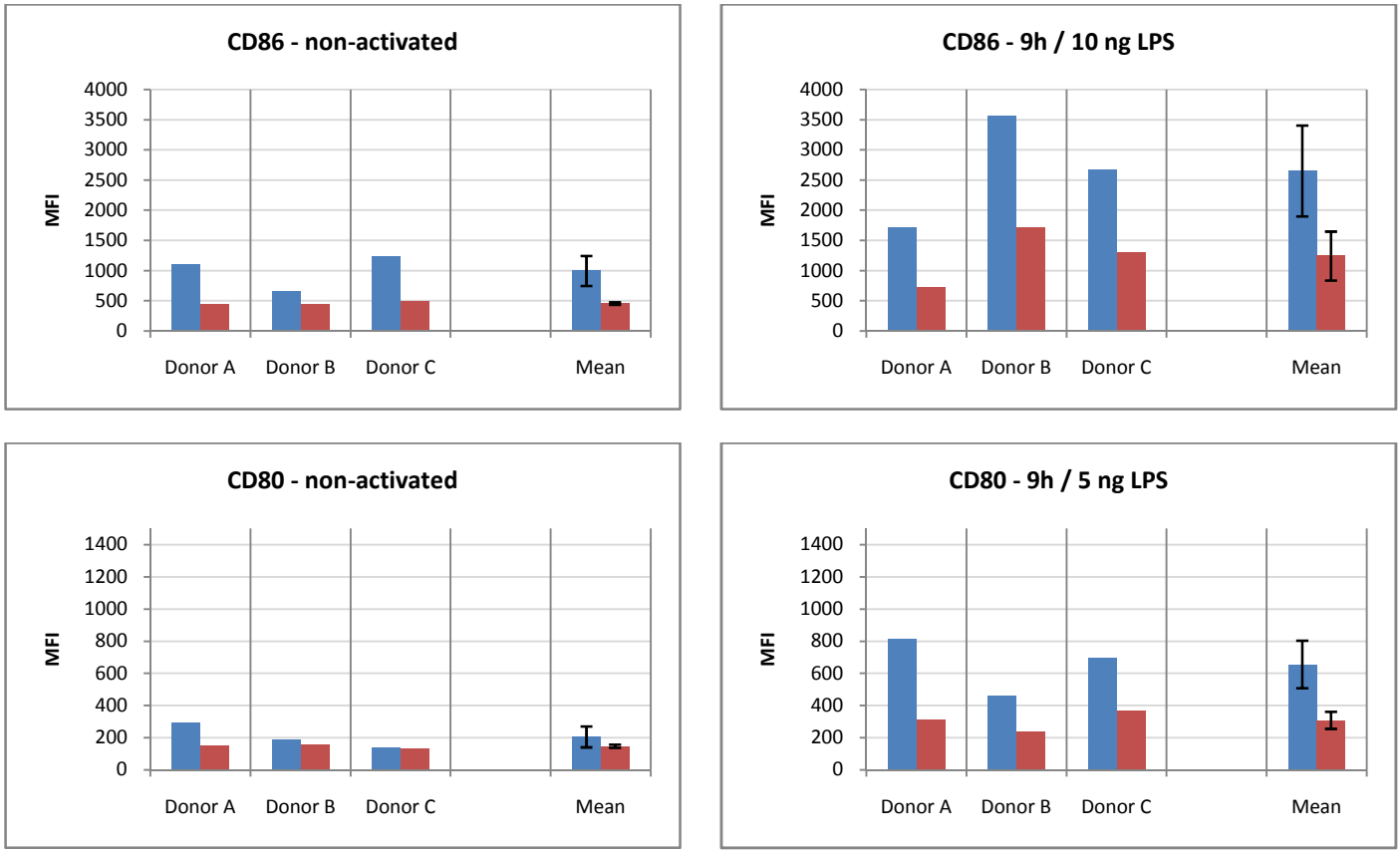

Mean fluorescence intensity (MFI) values measured for the costimulatory surface markers CD86 and CD80 for three independent donors in miR-181a knockdown (anti-mir-181a) vs. control vector (control) transfected dendritic cells under non-stimulated condition and after stimulation for 9 h with either 5 or 10 ng of LPS. Respective mean values of the three donors are displayed for each chart with error bars denoting standard deviation.

4.2. Increased cytokine secretion in miR-181a knockdown DCs

DCs are able to secrete a number of distinct cytokines and chemokines in their immature state as well as upon activation. These molecules are pivotal in sustaining a steady-state immune cell population of immune cells in the corresponding tissue, and for attracting other members of the immune system to the site of inflammation.

Figure 5. Cytokine secretion by miR-181a knockdown DCs

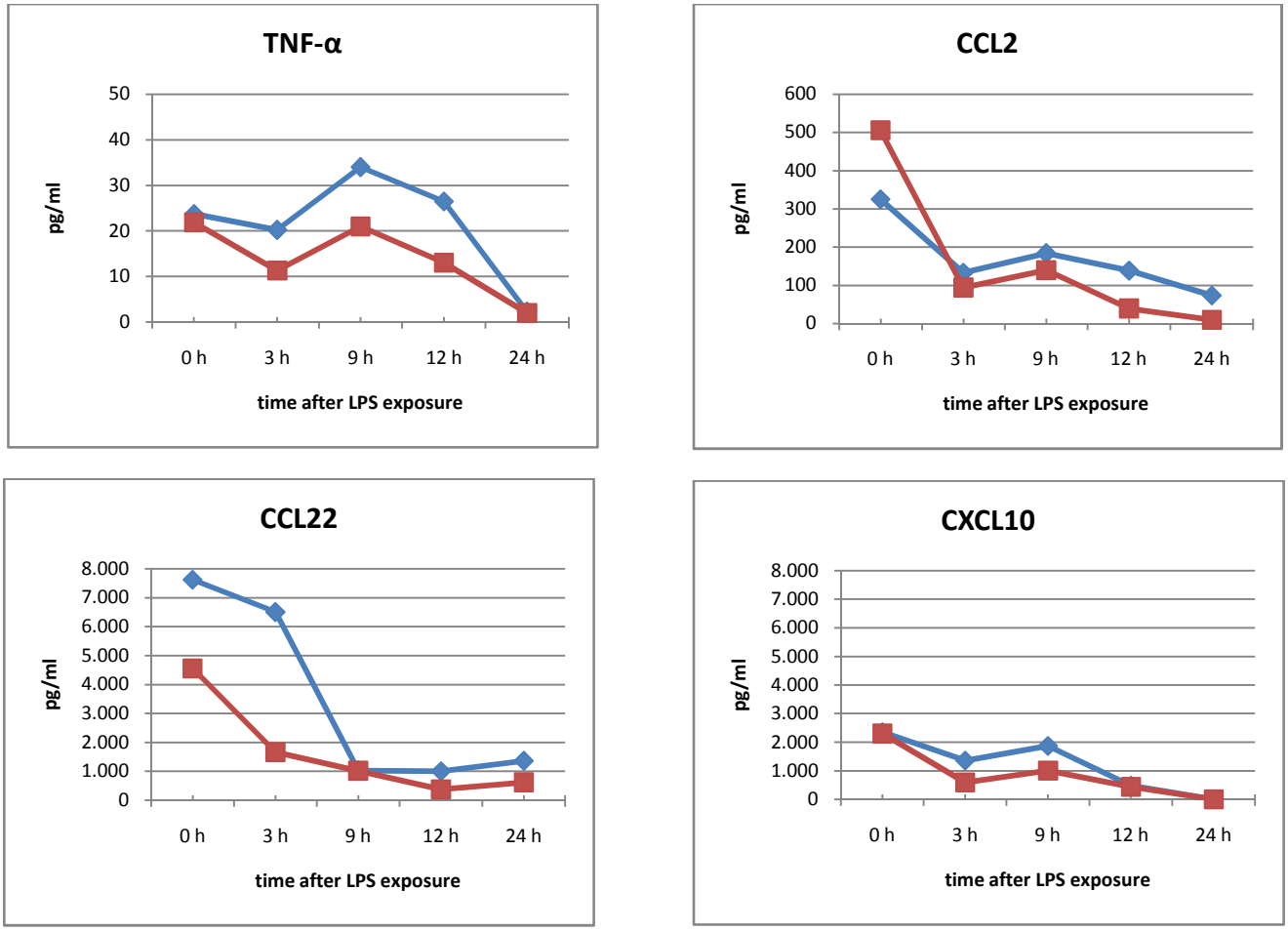

Cytokine secretion levels of knockdown (anti-mir-181a) vs. control vector (control) transfected dendritic cells under non-stimulated condition and after exposure to 10 ng LPS for 3 h, 9 h, 12 h and 24 h, respectively. Levels are measured in pg/ml, where 1 ml of the culture supernatant used in the analysis contained approx. 10^5 cells. Representative data from three independent donors is shown for each cytokine.

In addition to the upregulation of costimulatory molecules upon exposure to stimuli, the secretion of TNF-α, CCL2, CCL22 and CXCL10 was increased in the knockdown dendritic cells [Fig 5.]. Being one of the core cytokines produced by the immune system, tumor necrosis factor alpha (TNF-α) is ubiquitously expressed under inflammatory conditions by cells of the immune system as well as by a range of other cell types including fibroblasts, osteoclasts or smooth muscle cells, to name a few [61]. The protein is initially translated as membrane bound 26 kDa pro-TNF which is, subsequently,

cleaved into a soluble 17 kDa isoform by a metalloproteinase [62]. Monocytes and macrophages are the chief producers of soluble TNF-α and serum levels of the cytokine may directly be correlated to the severity of an inflammation or infectious disease [63, 64]. CCL2, also known as monocyte chemoattractant protein-1 (MCP-1), enacts a chemotactic effect on monocytes, natural killer cells and memory T-cells. The chemokine is responsible for the recruitment of these immune cells into inflammatory foci and it has been shown to aggravate inflammatory conditions and diseases [65, 66]. CCL22 (also known as MDC) is vividly expressed by DCs both in the immature state and after having received maturating stimuli. The chemokine instigates a strong chemotactic response in other DCs, natural killer cells and chronically activated T-cells, binding to the CCR4 chemokine receptor [67]. Exceptionally high DC-derived tissue expression levels of CCL22 have been detected in patients suffering from atopic dermatitis [68], an inflammatory skin. Besides, it was demonstrated in mice that CCL22 improved the capabilities of macrophages in the clearance of bacterial infections [69] and that antigen-pulsed DCs overexpressing CCL22 were able to induce a strong Th_2 response against the pathogen *Pseudomonas aeruginosa* [70]. CXCL10 was initially identified as an interferon-gamma induced inflammatory chemokine secreted by different cell types including monocytes and dendritic cells [71], and participation of CXCL10 in the aggravation of several autoimmune disorders has been implicated [72]. Our experimental panel also checked for changes in the secretion of the proinflammatory cytokines IL12 and IFN-γ, however, their concentrations in the culture supernatants were found to be below the detection threshold of the experimental setup (data not shown).

4.3. Increased motility towards lymphatic CCL19 cytokine gradient in miR-181a knockdown LPS-activated dendritic cells

Next, we asked whether the increased maturation observed would also lead to enhanced migratory capability of our miR-181a knockdown DCs. To determine the optimal conditions for monitoring the prospective increase in cell

migration we initially decided to test the cell migration assay with wildtype DCs. Based on the literature, DCs are expected to initiate their CCR7-driven migration approximately 3 hours after having received the stimulatory signal. In vivo, DCs then commonly reach their destination, the nearest afferent lymph node, after a period of roughly 24hours. Hence, we chose to perform the assay with wildtype DCs stimulated for 6 hours and 18 hours, respectively, with increasing concentrations of LPS. This experiment revealed a noticeable dose-dependent effect of the LPS concentration on the maximal total cell migration towards the CCL19 gradient [Fig 6.A]. Also, it appeared that LPS dosage solely influenced directional chemotaxis in the gradient in contrast to general migratory speed, as shown by the relative uniformity of the measured movement profiles perpendicular to the gradient's orientation. DCs stimulated for 18 hours achieved peak migration almost immediately at the beginning of the assay as opposed to 6 hours-stimulated cells. The generally observed decline in directional migration over time was ostensibly caused by dilution of the chemokine gradient in the 3D gel due to diffusion.

Based on the initial testing, we determined a concentration of 80 ng/ml LPS as optimal for the migration assay, as we had previously observed a decrease in cell viability at 100 ng/ml LPS, most likely due to overstimulation of the DCs (data not shown). Practical considerations regarding the activation procedure and availability of the time-lapse microscopes led us to set the activation time prior to the assay at 24 hours. Consequently, we detected a pronounced gain in the total chemotaxis towards increased chemokine concentrations in the miR-181a knockdown DC population compared to control vector-transfected cells. The knockdown of miR-181a resulted in improved speed of the total cell population along the vertical axis following the gradient; and a slightly increased movement profile of the knockdown DC population perpendicular to the gradient's axis was also detected [Fig 6.B]. Morphologically, both migrating knockdown and control DCs looked and acted identical upon microscopic examination.

DC migratory behavior is a complex mechanism characterized by alternating phases of scanning their microenvironment for the signal gradient through the formation of cytoplasmic protrusions and bursts of "flowing" amoeboid movement towards the increasing signal concentration detected [73]. Therefore, the observed improvement of migratory activity towards the CCL19 gradient of miR-181a knockdown DCs may occur either due to a straight increase in cellular movement speed or due to an intensified capability of sensing and following the chemokine gradient, resulting in a more directed movement pattern.

Figure 6. Chemotaxis profiles of mature DCs in 3D collagen matrix

A

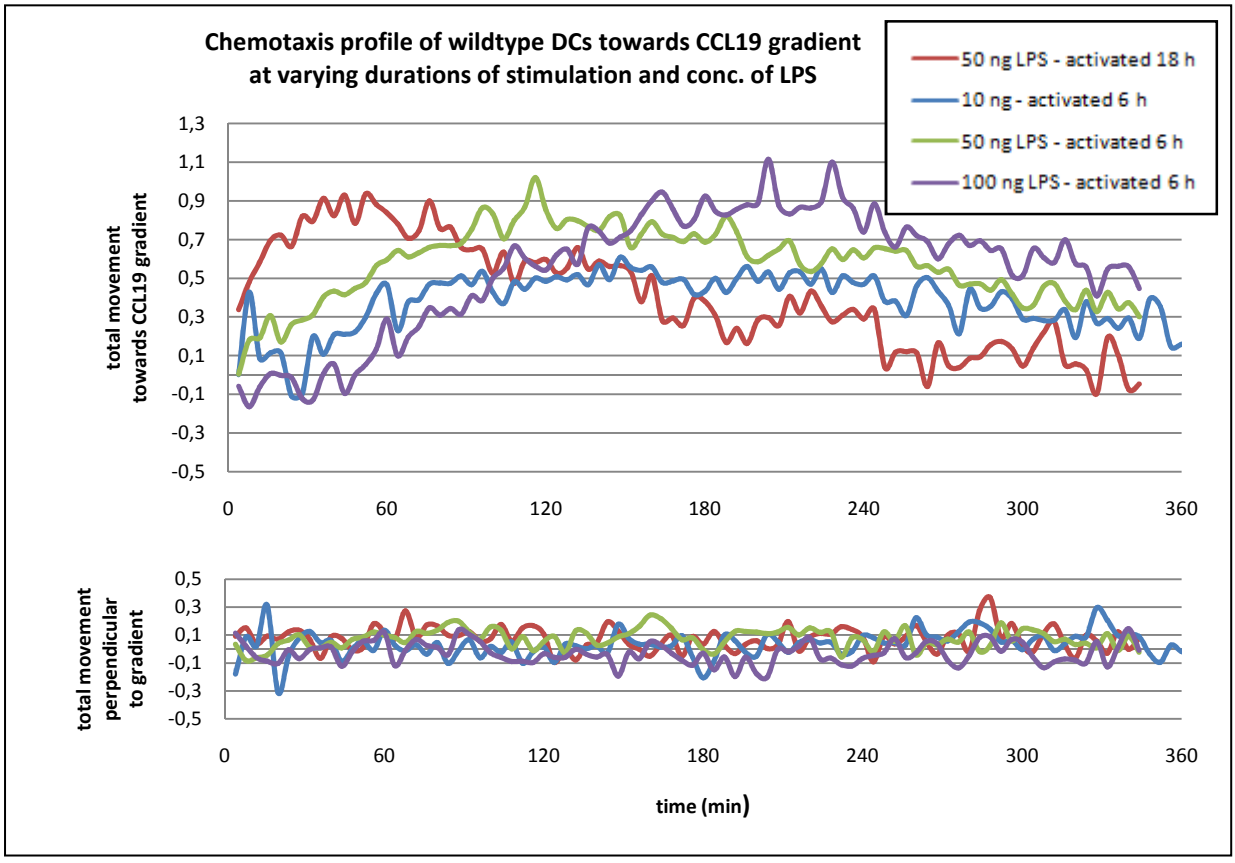

B

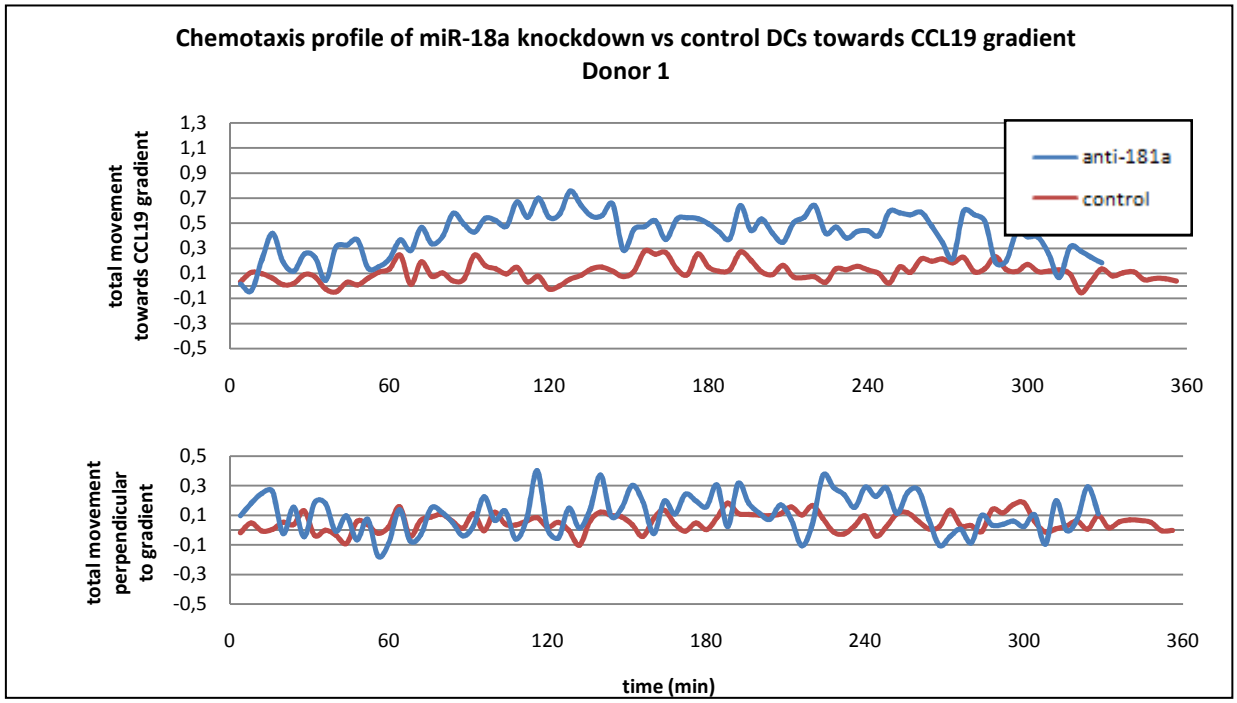

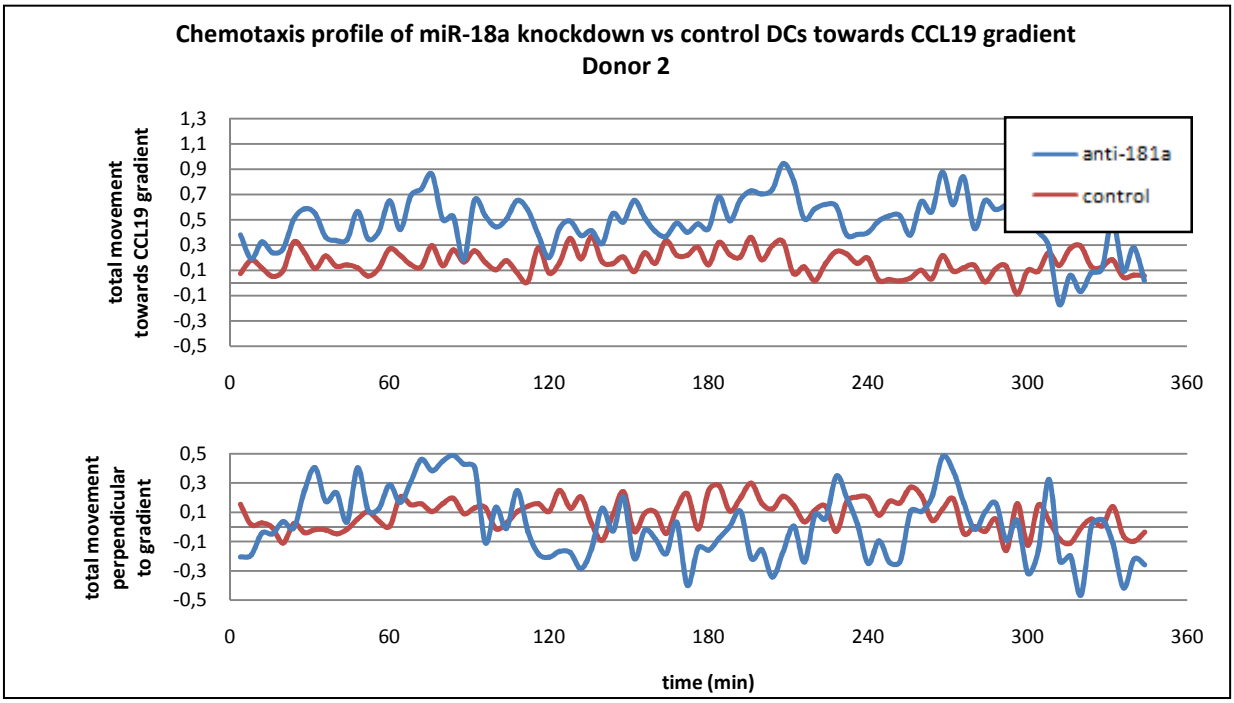

A) Chemotaxis profiles of miR-181a knockdown (anti-181a) vs. control vector (control) transfected mature DCs migrating in a CCL19 gradient, measuring the total displacement of the cells between each frame of the time-lapse microscope videos. For each profile, the upper chart represents total movement towards increasing concentration of CCL19 while the lower chart represents movement perpendicular to the gradient's axis. B) Chemotaxis profiles of wildtype mature DCs migrating in a CCL19 gradient, measuring the total displacement of the cells between each frame of the time-lapse microscope videos. For each profile, the upper chart represents total movement towards increasing concentration of CCL19 while the lower chart represents movement perpendicular to the gradient's axis.

Figure 7. Trajectories and analysis of DC chemotaxis towards CCL19 gradient

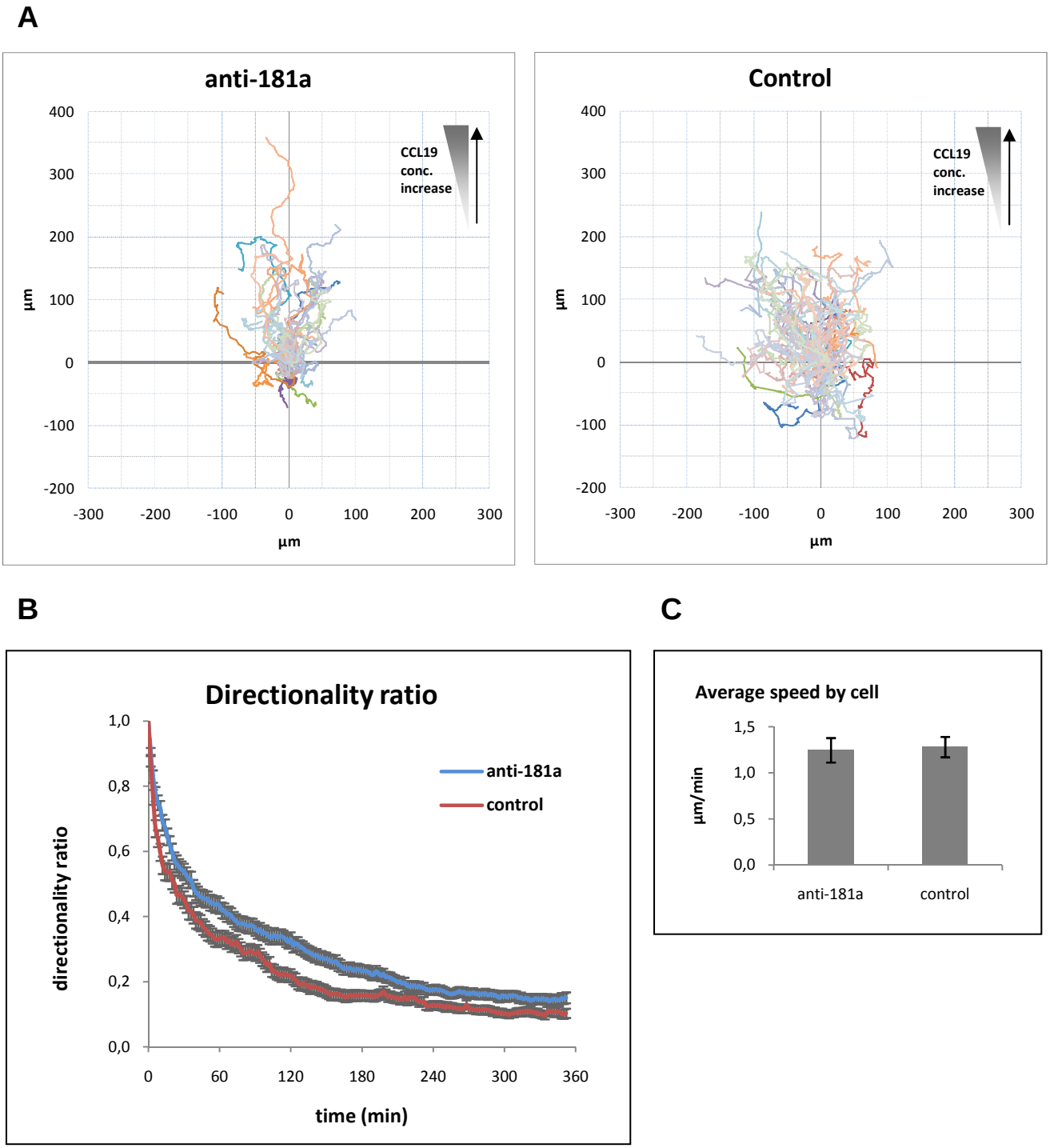

A) Normalized trajectories of mature DCs migrating in a CCL19 gradient, with 41 separate tracks for mir-181a knockdown DCs (anti-181a) and 63 separate tracks for control vector transfected DCs (control) overlaid, respectively. Starting points of each track are normalized at zero/zero coordinates. CCL19 gradient concentration increases towards positive y-values. B) Directionality ratio of miR-181a knockdown (anti-181a) vs. control vector (control) transfected mature DCs migrating in a CCL19 gradient, representing the mean values of 180 separate cells for each condition. Data is representative for three independent donors. C) Average cell speed in µm/min of miR-181a knockdown (anti-181a) vs. control vector (control) transfected mature DCs migrating in a CCL19 gradient. Data is representative for three independent donors.

Therefore, we tried to elucidate which mechanism facilitated the enhancement in chemotactic capacity. Plotting of the migration paths of miR-181a knockdown and control DCs demonstrated that the population of trajectories derived from knockdown DCs was visibly leaner along the axis perpendicular to the gradient's orientation and had a stronger tendency towards rising chemokine concentrations, as compared to control vector-transfected DCs [Fig 7.A]. In addition, our analysis revealed no effect of miR-181a knockdown on the average speed of the migrating DCs [Fig 7.C]. Instead, this study suggests that knockdown of miR-181a improves the efficiency of the cells in following the directional cues provided by the CCL19 gradient, as verified by the higher directionality ratio over time derived for the migrating miR-181a knockdown population [Fig 7.B].

4.4. Identification of direct miR-181a targets

Prior microarray analysis had identified more than 580 coding mRNAs significantly deregulated in day 3 differentiated DC precursors upon knockdown of miR-181a. Peculiarly, a major inconsistency in the expression levels obtained through the microarray was encountered, since one of the three donors tested (Donor 2) demonstrated radically opposite regulation in a considerable number of genes affected in the other two samples. A definite reason for this behavior could not be identified. Ruling out failure of the shRNA mediated knockdown or systemic error it may be theorized that a hitherto unknown donor-specific factor was activated by the loss of miR-181a repressive function, not only negating but counteracting one or several key effects of the microRNA knockdown. Provided the consistency of the changed mRNA levels of the other two donors (Donor 1 and Donor 3) with the phenotypic effects obtained by independent experiments, the candidate genes derived from the microarray data excluding Donor 2 were, nevertheless, considered promising enough to justify further analysis.

Figure 8. miR-181a controlled genes identified by Argonaute-2 RIP-ChIP and algorithm prediction of miR-181a binding sites

A

genesymbol	predictedby			fold increase (anti-181a vs. control)
	Target scan	MiRanda	Pictar	
CCL2				3.13
TMEM156				2.50
F3				2.27
OCSTAMP				2.18
CXCL10				2.15
ARHGAP42				1.99
CCL1				1.90
TNFRSF21				1.78
TTLL4				1.66
ITGA5				1.62
HDAC9		✓		1.59
ZNF93				1.59
SNAR-E				1.44
CD69	✓	✓		1.40
OGG1				1.39
EIF4EBP1				1.38
CFL2		✓		1.38
HIST1H2BK				1.38
DUSP7		✓		1.36
STXBP1				1.34
SASH3				1.34
DUSP18				1.33
PPARD				1.33
DUSP5	✓	✓	✓	1.32
BIRC3				1.32
FAM49A		✓		1.32
KCNN4				1.31
PPARG		✓		1.31
SLC17A5				1.30

genesymbol	predictedby			fold increase (anti-181a vs. control)
	Target scan	MiRanda	Pictar	
SEMA7A				1.30
CCRN4L				1.30
MICB				1.28
LINC00398				1.27
PPIL1				1.27
FNDC3B		✓	✓	1.27
ANXA2P1				1.27
RGCC				1.26
STX3				1.26
RBMS2				1.26
MYLIP				1.25
WDR62				1.25
PFKFB3				1.24
SH2B3	✓	✓		1.24
DUSP10		✓		1.23
GBA2		✓		1.23
DNM1P46				1.23
MICB				1.23
ZNFX1				1.23
GOLGA8J				1.23
APRT				1.22
TAOK2				1.22
TPRG1L				1.22
NHLRC2		✓		1.22
CH25H		✓		1.22
PNPLA6				1.22
HN1L				1.22
SMARCB1				1.21
PLAGL2				1.21

B

Example predicted binding structure of miR-181a to TNF-α mRNA

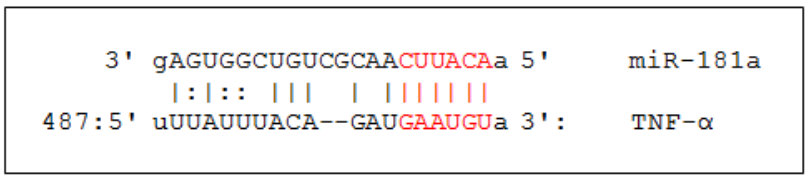

A) List of genes upgregulated in miR-181a knockdown day 3 DC precursors, verified as miR-181a targets by Argonaute2coimmunoprecipitate (RIP-ChIP). Fold increases are mean values of two separate donors. Check marks denote genes predicted as miR-181a targets by one or several of the three miR target identification algorithms used. B) Example predicted binding of human miR-181a 22nt sequence to the mature mRNA transcript of TNF-α. The section of DNA sequence shown for TNF-α starts at position 487 of the mRNA nucleotide sequence. Perfect nucleotide base pairing is denoted as "|",while ":" denotes wobble base pairing. Match of the miR-181a seed sequence required for recognition of the target mRNA is indicated in red. From MiRanda (http://www.microrna.org/).

To ascertain which mRNAs were upregulated directly due to the loss of repressive mir-181a function a microarray of mRNAs co-immunoprecipitated with the protein argonaute-2 (Ago2) had been performed earlier, expecting target mRNAs of miR-181a to be depleted in the precipitate after knocking down said microRNA; this method is also called ribonucleoprotein immunoprecipitation-microarray profiling or RIP-ChIP [74, 75].

By correlating the depleted mRNAs with the genes upregulated in the prior microarray a list of genes directly derepressed by the mir-181a knockdown could be obtained. These candidate genes were verified by comparison with a list of algorithm-predicted miR-181a targets [Fig 8.A]. In addition, the method identified a number of genes supposedly under miR-181a control but lacking considerable upregulation in the microarray. Still, the expression of these targets may be induced later into the differentiation process or during activation of the immature DCs, making these genes auspicious elements in our knockdown model.

4.5. Target genes of interest

Utilizing pathway prediction tools as well as extensive literature research, a number of genes of interest supposedly under direct miR-181a control were selected for further scrutiny from the candidates derived previously.

4.5.1. Dual specifity phosphatases

Threonine/serine phosphatases of the dual specifity phosphatase (DUSP) family are prominent regulators of intracellular signaling. Crucial in innate and adaptive immune response, DUSPs primarily target the MAPK family proteins ERK, JNK and p38 and may be broadly classified by their subcellular localization: cytosolic, nuclear or dually-located. By removing activating phosphate groups from MAPK proteins, DUSPs exert control over a large number of MAPK downstream targets, most being transcription factors.

Thus, DUSP class proteins are able to modulate the threshold for incoming stimuli relying on MAPK pathways. Additionally, DUSPs may act by competitive binding and sequestering substrates in their corresponding cellular compartments. DUSP expression is highly regulated and many downstream effectors of MAPKs specifically enhance the transcription of DUSP proteins, creating negative feedback loops tightly controlling the intensity and duration of intracellular signaling events [76-78].

The mRNAs of several DUSPs contain binding motifs for miR-181a. In particular, DUSP5 has been established to be controlled by mir-181a [46] and was identified to be depleted in the RIP-Chip. Furthermore, we also identified DUSP7 as another miR-181a controlled dual specifity phosphatase, with a moderate mRNA increase measured.

Both DUSP5 and DUSP7 (also known as PYST-2) are primarily ERK-specific MAPK phosphatases, the difference being that DUSP5 is localized in the nucleus while DUSP7 resides in the cytoplasm [79, 80]. Intriguingly, evidence has shown that one of the main inducing pathways for the expression of these phosphatases is the ERK signaling cascade itself. This results in the establishment of a negative feedback loop in the ERK pathway [81, 82].

ERK stimulation occurs in a broad variety of extracellular signaling events in both innate and adaptive immunity [83]. Negative regulation of the ERK pathway in monocytes and DCs has been associated with enhanced maturation, an increase in costimulatory surface markers and IL12 secretion as well a strong allostimulatory capacity [84, 85], while ERK overstimulation was found to impair maturation and to result in a more tolerogenic phenotype besides a general shift of immune activation towards the humoral Th2 response [85, 86].

4.5.2. Tumor necrosis factor alpha

Significant depletion of TNF-α mRNA was measured by RIP-ChIP and the cytokine's mRNA sequence incorporates at least one conserved strong miR-181a binding site [Fig 8.A]. Elevated levels of TNF-α secretion were detected in LPS-stimulated miR-181a knockdown DCs [Fig 5.]. Heightened autocrine TNF-α signaling may at least partially explain the improved maturation markers observed upon knockdown of miR-181a. TNF-α is a primary, ubiquitously expressed inflammatory cytokine. An increase of TNF-α expression through the direct effect of miR-181a substantiates the proposed role of miR-181a as a tuning mechanism against runaway immune reactions.

4.6. MAPK activity in miR-181a knockdown DCs after LPS stimulation

The regulation of several DUSPs by miR-181a implicates alterations in MAPK signaling in our miR-181a knockdown DCs. As the repressive regulation of DUSPs through miR-181a is alleviated, a decrease in MAPK phosphorylation levels may be expected, particularly in regards to ERK phosphorylation through the actions of the miR-181a targets DUSP5 and DUSP7. The impact of impaired MAPK signaling on DCs has been briefly described earlier (see paragraph 4.5.1.). As DUSP expression is chiefly driven by the negative feedback loops from the MAPK signaling pathways, we decided to examine ERK, JNK and p38 phosphorylation levels after the cells having received a strong external stimulus able to trigger all three MAPK pathways, in our case through stimulation with LPS, which was expected to immediately induce a sharp peak in MAPK phosphorylation. Afterwards, the levels of phosphorylated MAPK were to quickly decline as the initial signal is cut off by the action of MAPK phosphatases, including DUSP class proteins.

Figure 9. Differential MAPK activation after LPS stimulation in miR-181a knockdown vs. control DCs

A **Relative MAPK phosphorylation levels after stimulation with 100 ng LPS**

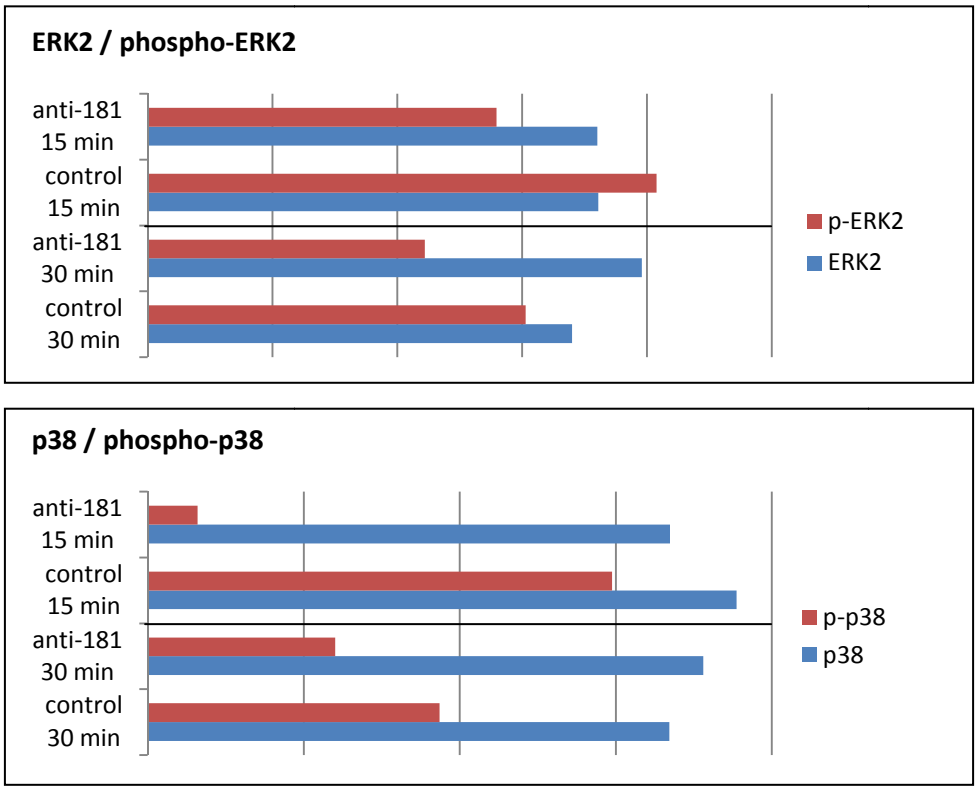

B **Western blot - MAPK phosphorylation after stimulation with 100 ng LPS**

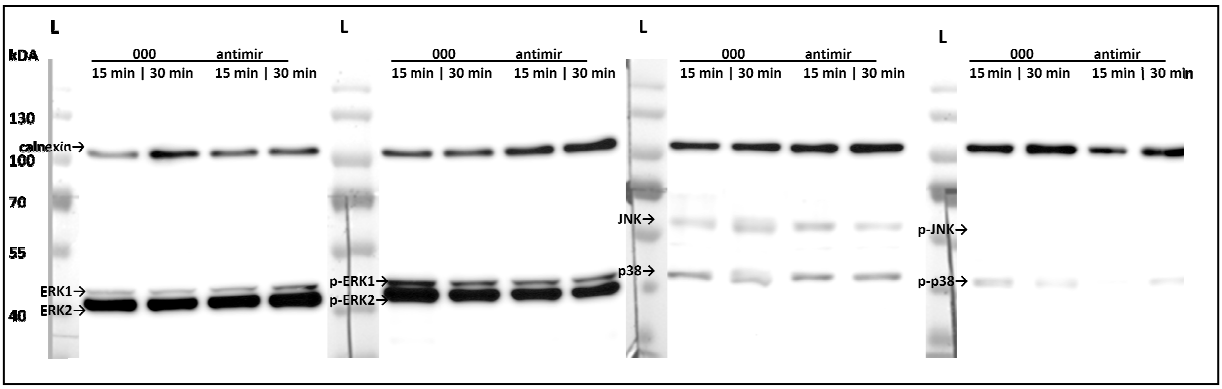

A) Relative levels of both total (blue) and phosphorylated (red) MAPKs ERK 1/2 and p38 at indicated time points after stimulation of miR-181a knockdown vs. control vector-transfected DCs with 100 ng LPS, as determined by Western blot (measuring the intensity of the lanes, normalized by the levels of calnexin as loading standard). B) Western blot of the MAPKs ERK 1/2, p38 and JNK, both for total and phosphorylated levels after stimulation of DCs with 100 ng LPS for 15 min and 30 min, respectively. Antibody specifity for phosphorylated MAPKs is against phosphorylation at Thr202/Tyr204 for ERK 1/2, Thr180/Tyr182 for p38 and Thr183/Tyr185 for JNK. Calnexin was used as loading standard. PageRuler Prestained Protein Ladder was used as ruler (lanes denoted as "L").

Western blot for the MAPKs ERK, JNK and p38 as well as their respective phosphorylated versions was performed for the lysates of miR-181a knockdown and control vector-transfected DCs after stimulation with LPS [Fig 9.A]. In accordance with previous studies, rapid phosphorylation of the MAPKs ERK1/2 and p38 could be detected minutes after stimulation of the DCs with LPS; phospho-JNK was not detectable in our assay. The experiment determined the levels of phospho-ERK2 to be reduced by approximately 30 % in miR-181a knockdown DCs [Fig 9.B]. In addition, a repressive effect of miR-181a knockdown on the levels of phospho-p38 was observable, indicating both a decrease in overall phospho-p38 as well as apparently delayed kinetics in p38 pathway activation. However, in order to determine the exact effect of miR-181a knockdown on p38 kinetics, comparative observation of the levels of phospho-p38 over a longer time interval would be warranted. MAPKs are governed by a complex network of crosstalk mechanisms, and alterations in ERK activation alone may trigger a cascade of changes in other members of the MAPK family.

4.7. Lentiviral transduction of peripheral blood mononuclear cells

In addition to understanding the effect of endogenous expression of miR-181a on the activation of DCs (using our human cord blood-derived CD34+ dendritic cell culture system), another important aspect of this thesis was to optimize a protocol to knock down the microRNA in peripheral blood monocyte (PBMC)-derived CD14+ DCs. In vivo, circulating PBMCs are recruited into sites of active inflammation where they may differentiate into a subset of DCs called monocyte-derived DCs (moDCs). These cells represent a distinct subclass of DCs, sharing characteristics with both conventional DCs and macrophages on a molecular level [87]. The collection, maintenance and differentiation of PBMCs is less involved and yields higher numbers of cells as compared to CD34+ cord blood-derived cells, making a CD14+ DC model system attractive; peripheral blood is easier to come by, high numbers of cells can reliably be isolated and their differentiation into DCs requires less time and cytokines than CD34+ DCs.

However, PBMCs possess strong natural resistance to lentiviral infection, thus requiring excessive amounts of viral particles to obtain useful transduction rates; in fact, the viral payload necessary is big enough to affect the viability of the cells and skew experimental results. Fortunately, there exists an alternative to employing copious amounts of lentiviral particles in order to transduce PBMCs. PBMC resistance to lentiviruses relies on SAMHD1, a protein capable of hydrolyzing intracellular deoxynucleoside triphosphates (dNTPs), lowering their concentrations to below those required for the synthesis of the viral DNA by reverse transcriptase [88]. HIV-1-derived lentiviral vectors, such as the one used in this study, are incapable of overcoming this resistance.

Nevertheless, simian immunodeficiency viruses (SIVs) maintain a variant of their Vpx gene able to inhibit the activity of SAMHD1, a function that was lost when the virus crossed over to human hosts. By supplementing the infectious lentiviral vector with non-infectious SIV "helper" virion-like particles carrying this particular Vpx variant, the resistance of PBMCs can be broken [89]. The addition of SIV virion-like particles allows to achieve high transduction rates in PBMCs with lentiviral payloads comparable to those employed in the transduction of CD34+ cord blood-derived hematopoietic stem cells.

Addition of SIV virion-like particles during the lentiviral transduction of PBMCs led to a drastic increase in successfully transduced cells compared to using the lentiviral vector alone; with the support from the SIV virion transduction rates comparable to those for CD34+ cells could be obtained when using the same amounts of lentiviral vector [Figure 9]. The ideal dilution ratio for fresh SIV virion-like particle-containing supernatant in lentiviral vector supernatant was determined to be 1:5, allowing a stable transduction rate in excess of 90 % of the cells. This method allows one to reliably produce useful numbers of transduced CD14+ PBMC-derived DCs within a shorter period of time and with less use of cytokines. Whether the knock-down of miR-181 in these peripheral blood moDC would lead to similar phenotypic changes as in CD34-derived dendritic cells is to be determined.

Figure 10. Lentiviral transduction of CD14+ PBMCs aided by SIV helper virions

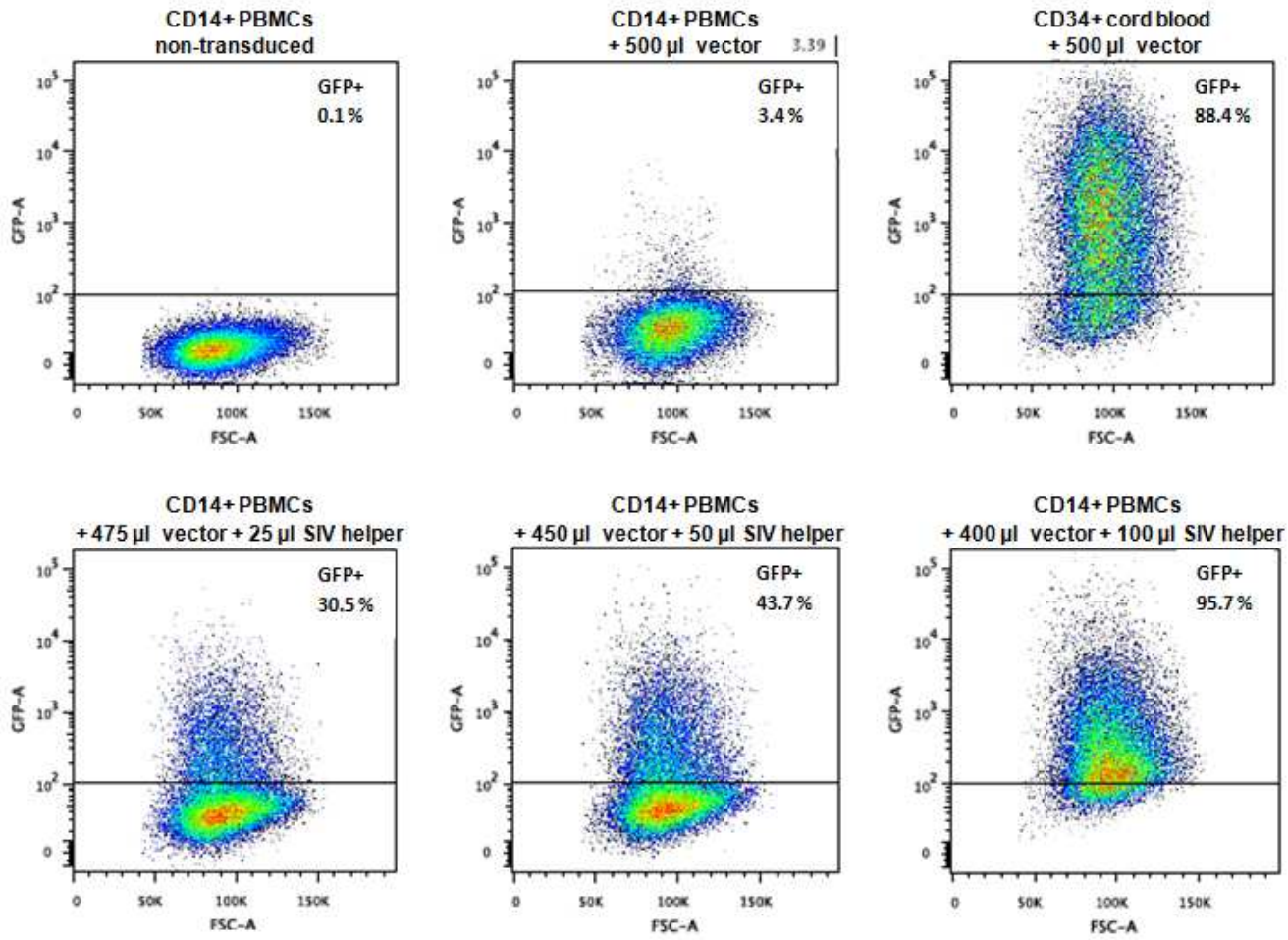

Transduction of CD14+ PBMCs with lentiviral GFP+ " control plasmid (vector) using varying amounts of SIV helper virion-like particles (SIV helper). Fresh, filtered viral culture supernatants were directly used in the transduction, with the corresponding volumes given. No second round of infection was performed. Percentages of GFP positive cells measured by FACS after transduction are indicated.

5. Discussion

It could be shown that knockdown of the microRNA miR-181a in human dendritic cells results in a more mature, more inflammatory phenotype, as demonstrated by the increased proinflammatory cytokine production, heightened costimulatory receptor levels and improved chemotactic capability after activation of the cells that has been detected. These results are in accordance with our initial theory of miR-181a playing a role in regulating the magnitude of inflammatory reactions through the modulation of dendritic cell activity, mainly by altering their capability to elicit an adaptive immune response. As discussed earlier, miR-181a expression was found to be upregulated in lymphocytes in vivo as a response to inflammatory settings, likely to prevent excessive immune response and "off-target effects" in the form of spontaneous immune activation against otherwise harmless antigens [54-56].

The inflammatory cytokine TNF-α, among other signaling molecules, is a prime target of miR-181a. Autocrine TNF-α signaling certainly propagates the increase in maturation markers in miR-181a knockdown DCs. The fact that the microRNA is able to restrain TNF-α expression strongly reinforces the view of miR-181a being a crucial regulator of immune responses. In addition, the observed decrease in MAPK signaling, specifically in ERK phosphorylation levels [Fig 9.], upon LPS stimulation may contribute to the inflammatory phenotype of miR-181a knockdown DCs. Impairment of ERK signaling has previously been shown to facilitate DC maturation [84, 85]. Presumably, this mechanism is facilitated mainly by the miR-181a target DUSP5, besides other members of the dual specifity phosphatase family supposedly targeted by this microRNA. As the ERK-repressor DUSP5 is expressed in response to ERK stimulation, thus creating a negative feedback loop in the signaling pathway [81], mitigating the repression of DUSP5 mRNA by miR-181a knockdown may be expected to result in both higher DUSP5 steady-state levels and, consequently, an increased ERK activation threshold as well as in a swifter shutdown of ERK signaling upon acute stimulation of the pathway. In reverse, repression of DUSP5 expression by miR-181a would blunt the aforementioned

negative feedback in ERK signaling, thus aggravating the negative effects of ERK on DC maturation; this mechanism, as well as the above-mentioned repression of TNF-α, conform with one of the suggested physiological roles of miR-181a as a failsafe against over-stimulation of the immune system under inflammatory conditions [56].

In conjunction with the modulation of intracellular signaling pathways like ERK, miR-181a may further affect the immunological outcome of DC activation through alteration of their migratory capabilities. Following DC activation and antigen uptake, chemotactic movement towards the lymphatic system – and, ultimately, stimulation of lymphoid-resident T cells – remains a most crucial step in mounting an adaptive immune response. Our study could convincingly demonstrate changes in the chemotactic capacity of miR-181a knockdown DCs [Fig 6. / Fig 7.]. Although not enhancing the absolute movement speed of DCs, suppression of miR-181a was shown to intensify the directionality of DC migration towards the lymphatic chemokine CCL19. In vivo, an increased ability of DCs to effectively home towards lymphatic chemokine cues may as well improve their success rate in reaching a peripheral lymph node, thus enabling them to evoke an adaptive immune response through T cell stimulation.

This study demonstrates that miR-181a plays a pivotal role in tuning the activity and responsiveness of dendritic cells, the "sentinels" of the immune system in their function as primary antigen presenting cells. Through adjustment of APC activity miR-181a is able to apply fine control over the downstream immune cascade in both the innate and adaptive compartment. miR-181a operates on several functional layers of DC biology, ranging from intracellular signaling pathways over cytokine production to chemotactic migration, thus providing a diverse instrument for the immune system to calibrate the occurrence and severity of inflammatory reactions at the initial, crucial steps of antigen recognition and presentation.

6. Bibliography

1. Steinman, R.M. and Z.A. Cohn, *Identification of a novel cell type in peripheral lymphoid organs of mice. I. Morphology, quantitation, tissue distribution.* J Exp Med, 1973. **137**(5): p. 1142-62.
2. Shortman, K. and Y.-J. Liu, *Mouse and human dendritic cell subtypes.* Nat Rev Immunol, 2002. **2**(3): p. 151-161.
3. Moore, A.J. and M.K. Anderson, *Dendritic Cell Development: A Choose-Your-Own-Adventure Story.* Advances in Hematology, 2013. **2013**: p. 16.
4. Shortman, K. and S.H. Naik, *Steady-state and inflammatory dendritic-cell development.* Nat Rev Immunol, 2007. **7**(1): p. 19-30.
5. McKenna, H.J., et al., *Mice lacking flt3 ligand have deficient hematopoiesis affecting hematopoietic progenitor cells, dendritic cells, and natural killer cells.* Blood, 2000. **95**(11): p. 3489-97.
6. Karsunky, H., et al., *Flt3 ligand regulates dendritic cell development from Flt3+ lymphoid and myeloid-committed progenitors to Flt3+ dendritic cells in vivo.* J Exp Med, 2003. **198**(2): p. 305-13.
7. D'Amico, A. and L. Wu, *The early progenitors of mouse dendritic cells and plasmacytoid predendritic cells are within the bone marrow hemopoietic precursors expressing Flt3.* J Exp Med, 2003. **198**(2): p. 293-303.
8. Schmid, M.A., et al., *Instructive cytokine signals in dendritic cell lineage commitment.* Immunological Reviews, 2010. **234**(1): p. 32-44.
9. Banchereau, J. and R.M. Steinman, *Dendritic cells and the control of immunity.* Nature, 1998. **392**(6673): p. 245-252.
10. Ferrero, I., O. Michelin, and I. Luescher, *Antigen Recognition by T Lymphocytes*, in *eLS*. 2001, John Wiley & Sons, Ltd.
11. Chung, C.Y., et al., *Dendritic cells: cellular mediators for immunological tolerance.* Clin Dev Immunol, 2013. **2013**: p. 972865.
12. Ganguly, D., et al., *The role of dendritic cells in autoimmunity.* Nat Rev Immunol, 2013. **13**(8): p. 566-577.
13. Akira, S., S. Uematsu, and O. Takeuchi, *Pathogen Recognition and Innate Immunity.* Cell. **124**(4): p. 783-801.
14. Matzinger, P., *An innate sense of danger.* Seminars in Immunology, 1998. **10**(5): p. 399-415.
15. Takeuchi, O. and S. Akira, *Pattern recognition receptors and inflammation.* Cell, 2010. **140**(6): p. 805-20.
16. Akira, S. and H. Hemmi, *Recognition of pathogen-associated molecular patterns by TLR family.* Immunology Letters, 2003. **85**(2): p. 85-95.
17. Granucci, F., et al., *Early events in dendritic cell maturation induced by LPS.* Microbes and Infection, 1999. **1**(13): p. 1079-1084.
18. Sozzani, S., et al., *Differential regulation of chemokine receptors during dendritic cell maturation: a model for their trafficking properties.* J Immunol, 1998. **161**(3): p. 1083-6.
19. Förster, R., et al., *CCR7 Coordinates the Primary Immune Response by Establishing Functional Microenvironments in Secondary Lymphoid Organs.* Cell. **99**(1): p. 23-33.
20. Ackerman, A.L. and P. Cresswell, *Regulation of MHC Class I Transport in Human Dendritic Cells and the Dendritic-Like Cell Line KG-1.* The Journal of Immunology, 2003. **170**(8): p. 4178-4188.
21. Villadangos, J.A., P. Schnorrer, and N.S. Wilson, *Control of MHC class II antigen presentation in dendritic cells: a balance between creative and destructive forces.* Immunological Reviews, 2005. **207**(1): p. 191-205.
22. Lee, R.C., R.L. Feinbaum, and V. Ambros, *The C. elegans heterochronic gene lin-4 encodes small RNAs with antisense complementarity to lin-14.* Cell, 1993. **75**(5): p. 843-854.

23. Lee, R., R. Feinbaum, and V. Ambros, *A short history of a short RNA.* Cell, 2004. **116**(2 Suppl): p. S89-92, 1 p following S96.
24. Hamilton, A.J. and D.C. Baulcombe, *A Species of Small Antisense RNA in Posttranscriptional Gene Silencing in Plants.* Science, 1999. **286**(5441): p. 950-952.
25. Fire, A., et al., *Potent and specific genetic interference by double-stranded RNA in Caenorhabditis elegans.* Nature, 1998. **391**(6669): p. 806-11.
26. Cerutti, H. and J.A. Casas-Mollano, *On the origin and functions of RNA-mediated silencing: from protists to man.* Curr Genet, 2006. **50**(2): p. 81-99.
27. Buchon, N. and C. Vaury, *RNAi: a defensive RNA-silencing against viruses and transposable elements.* Heredity (Edinb), 2006. **96**(2): p. 195-202.
28. Bernstein, E., et al., *Role for a bidentate ribonuclease in the initiation step of RNA interference.* Nature, 2001. **409**(6818): p. 363-6.
29. Hammond, S.M., et al., *An RNA-directed nuclease mediates post-transcriptional gene silencing in Drosophila cells.* Nature, 2000. **404**(6775): p. 293-6.
30. Gregory, R.I., T.P. Chendrimada, and R. Shiekhattar, *MicroRNA biogenesis: isolation and characterization of the microprocessor complex.* Methods Mol Biol, 2006. **342**: p. 33-47.
31. Verdel, A., et al., *RNAi-mediated targeting of heterochromatin by the RITS complex.* Science, 2004. **303**(5658): p. 672-6.
32. Chen, K. and N. Rajewsky, *The evolution of gene regulation by transcription factors and microRNAs.* Nat Rev Genet, 2007. **8**(2): p. 93-103.
33. Dostie, J., et al., *Numerous microRNPs in neuronal cells containing novel microRNAs.* RNA, 2003. **9**(2): p. 180-6.
34. Lagos-Quintana, M., et al., *New microRNAs from mouse and human.* RNA, 2003. **9**(2): p. 175-9.
35. Lim, L.P., et al., *Vertebrate microRNA genes.* Science, 2003. **299**(5612): p. 1540.
36. Bentwich, I., et al., *Identification of hundreds of conserved and nonconserved human microRNAs.* Nat Genet, 2005. **37**(7): p. 766-770.
37. Friedman, R.C., et al., *Most mammalian mRNAs are conserved targets of microRNAs.* Genome Res, 2009. **19**(1): p. 92-105.
38. He, L. and G.J. Hannon, *MicroRNAs: small RNAs with a big role in gene regulation.* Nat Rev Genet, 2004. **5**(7): p. 522-31.
39. Chen, C.Z., et al., *MicroRNAs modulate hematopoietic lineage differentiation.* Science, 2004. **303**(5654): p. 83-6.
40. O'Carroll, D., et al., *A Slicer-independent role for Argonaute 2 in hematopoiesis and the microRNA pathway.* Genes Dev, 2007. **21**(16): p. 1999-2004.
41. Baltimore, D., et al., *MicroRNAs: new regulators of immune cell development and function.* Nat Immunol, 2008. **9**(8): p. 839-45.
42. Sonkoly, E., M. Stahle, and A. Pivarcsi, *MicroRNAs and immunity: novel players in the regulation of normal immune function and inflammation.* Semin Cancer Biol, 2008. **18**(2): p. 131-40.
43. Guimaraes-Sternberg, C., et al., *MicroRNA modulation of megakaryoblast fate involves cholinergic signaling.* Leuk Res, 2006. **30**(5): p. 583-95.
44. Debernardi, S., et al., *MicroRNA miR-181a correlates with morphological sub-class of acute myeloid leukaemia and the expression of its target genes in global genome-wide analysis.* Leukemia, 2007. **21**(5): p. 912-6.
45. Ciafre, S.A., et al., *Extensive modulation of a set of microRNAs in primary glioblastoma.* Biochem Biophys Res Commun, 2005. **334**(4): p. 1351-8.
46. Li, Q.J., et al., *miR-181a is an intrinsic modulator of T cell sensitivity and selection.* Cell, 2007. **129**(1): p. 147-61.
47. Ebert, P.J., et al., *An endogenous positively selecting peptide enhances mature T cell responses and becomes an autoantigen in the absence of microRNA miR-181a.* Nat Immunol, 2009. **10**(11): p. 1162-9.

48. Krutzfeldt, J., et al., *Silencing of microRNAs in vivo with 'antagomirs'.* Nature, 2005. **438**(7068): p. 685-9.
49. Luo, L., et al., *Functional analysis of alloreactive memory CD4+ T cells derived from skin transplantation recipient and naive CD4+ T cells derived from untreated mice.* J Surg Res, 2012. **176**(2): p. 649-56.
50. Zietara, N., et al., *Critical role for miR-181a/b-1 in agonist selection of invariant natural killer T cells.* Proc Natl Acad Sci U S A, 2013. **110**(18): p. 7407-12.
51. Cichocki, F., et al., *Cutting edge: microRNA-181 promotes human NK cell development by regulating Notch signaling.* J Immunol, 2011. **187**(12): p. 6171-5.
52. Henao-Mejia, J., et al., *The microRNA miR-181 is a critical cellular metabolic rheostat essential for NKT cell ontogenesis and lymphocyte development and homeostasis.* Immunity, 2013. **38**(5): p. 984-97.
53. Hulsmans, M., et al., *Decreased miR-181a expression in monocytes of obese patients is associated with the occurrence of metabolic syndrome and coronary artery disease.* J Clin Endocrinol Metab, 2012. **97**(7): p. E1213-8.
54. Wu, C., et al., *microRNA-181a represses ox-LDL-stimulated inflammatory response in dendritic cell by targeting c-Fos.* J Lipid Res, 2012. **53**(11): p. 2355-63.
55. Xie, W., et al., *MiR-181a regulates inflammation responses in monocytes and macrophages.* PLoS One, 2013. **8**(3): p. e58639.
56. Xie, W., et al., *miR-181a and inflammation: miRNA homeostasis response to inflammatory stimuli in vivo.* Biochemical and Biophysical Research Communications, 2013. **430**(2): p. 647-652.
57. Jurkin, J., et al., *miR-146a is differentially expressed by myeloid dendritic cell subsets and desensitizes cells to TLR2-dependent activation.* J Immunol, 2010. **184**(9): p. 4955-65.
58. Shklovskaya, E., et al., *Langerhans cells are precommitted to immune tolerance induction.* Proc Natl Acad Sci U S A, 2011. **108**(44): p. 18049-54.
59. van der Aar, A.M., et al., *Langerhans cells favor skin flora tolerance through limited presentation of bacterial antigens and induction of regulatory T cells.* J Invest Dermatol, 2013. **133**(5): p. 1240-9.
60. Gorelik, R. and A. Gautreau, *Quantitative and unbiased analysis of directional persistence in cell migration.* Nat. Protocols, 2014. **9**(8): p. 1931-1943.
61. Bradley, J.R., *TNF-mediated inflammatory disease.* The Journal of Pathology, 2008. **214**(2): p. 149-160.
62. Black, R.A., et al., *A metalloproteinase disintegrin that releases tumour-necrosis factor-alpha from cells.* Nature, 1997. **385**(6618): p. 729-33.
63. Robak, T., A. Gladalska, and H. Stepien, *The tumour necrosis factor family of receptors/ligands in the serum of patients with rheumatoid arthritis.* Eur Cytokine Netw, 1998. **9**(2): p. 145-54.
64. Waage, A., A. Halstensen, and T. Espevik, *Association between tumour necrosis factor in serum and fatal outcome in patients with meningococcal disease.* Lancet, 1987. **1**(8529): p. 355-7.
65. Deshmane, S.L., et al., *Monocyte Chemoattractant Protein-1 (MCP-1): An Overview.* J Interferon Cytokine Res, 2009. **29**(6): p. 313-26.
66. Melgarejo, E., et al., *Monocyte chemoattractant protein-1: a key mediator in inflammatory processes.* Int J Biochem Cell Biol, 2009. **41**(5): p. 998-1001.
67. Vulcano, M., et al., *Dendritic cells as a major source of macrophage-derived chemokine/CCL22 in vitro and in vivo.* European Journal of Immunology, 2001. **31**(3): p. 812-822.
68. Hashimoto, S., et al., *Macrophage-derived chemokine (MDC)/CCL22 produced by monocyte derived dendritic cells reflects the disease activity in patients with atopic dermatitis.* Journal of Dermatological Science, 2006. **44**(2): p. 93-99.
69. Matsukawa, A., et al., *Pivotal Role of the CC Chemokine, Macrophage-Derived Chemokine, in the Innate Immune Response.* The Journal of Immunology, 2000. **164**(10): p. 5362-5368.

70. Kikuchi, T. and R.G. Crystal, *Antigen-pulsed dendritic cells expressing macrophage-derived chemokine elicit Th2 responses and promote specific humoral immunity.* J Clin Invest, 2001. **108**(6): p. 917-27.
71. Luster, A.D. and J.V. Ravetch, *Biochemical characterization of a gamma interferon-inducible cytokine (IP-10).* The Journal of Experimental Medicine, 1987. **166**(4): p. 1084-1097.
72. Lee, E.Y., Z.-H. Lee, and Y.W. Song, *CXCL10 and autoimmune diseases.* Autoimmunity Reviews, 2009. **8**(5): p. 379-383.
73. Heuze, M.L., et al., *Migration of dendritic cells: physical principles, molecular mechanisms, and functional implications.* Immunol Rev, 2013. **256**(1): p. 240-54.
74. Keene, J.D., J.M. Komisarow, and M.B. Friedersdorf, *RIP-Chip: the isolation and identification of mRNAs, microRNAs and protein components of ribonucleoprotein complexes from cell extracts.* Nat Protoc, 2006. **1**(1): p. 302-7.
75. Wang, W.X., et al., *Anti-Argonaute RIP-Chip shows that miRNA transfections alter global patterns of mRNA recruitment to microribonucleoprotein complexes.* Rna, 2010. **16**(2): p. 394-404.
76. Lang, R., M. Hammer, and J. Mages, *DUSP meet immunology: dual specificity MAPK phosphatases in control of the inflammatory response.* J Immunol, 2006. **177**(11): p. 7497-504.
77. Huang, C.Y. and T.H. Tan, *DUSPs, to MAP kinases and beyond.* Cell Biosci, 2012. **2**(1): p. 24.
78. Arthur, J.S.C. and S.C. Ley, *Mitogen-activated protein kinases in innate immunity.* Nat Rev Immunol, 2013. **13**(9): p. 679-692.
79. Mandl, M., D.N. Slack, and S.M. Keyse, *Specific inactivation and nuclear anchoring of extracellular signal-regulated kinase 2 by the inducible dual-specificity protein phosphatase DUSP5.* Mol Cell Biol, 2005. **25**(5): p. 1830-45.
80. Dowd, S., A.A. Sneddon, and S.M. Keyse, *Isolation of the human genes encoding the pyst1 and Pyst2 phosphatases: characterisation of Pyst2 as a cytosolic dual-specificity MAP kinase phosphatase and its catalytic activation by both MAP and SAP kinases.* J Cell Sci, 1998. **111 (Pt 22)**: p. 3389-99.
81. Kucharska, A., et al., *Regulation of the inducible nuclear dual-specificity phosphatase DUSP5 by ERK MAPK.* Cell Signal, 2009. **21**(12): p. 1794-805.
82. Levy-Nissenbaum, O., et al., *Dual-specificity phosphatase Pyst2-L is constitutively highly expressed in myeloid leukemia and other malignant cells.* Oncogene, 0000. **22**(48): p. 7649-7660.
83. Zhang, Y.L. and C. Dong, *MAP kinases in immune responses.* Cell Mol Immunol, 2005. **2**(1): p. 20-7.
84. Puig-Kröger, A., et al., *Extracellular signal–regulated protein kinase signaling pathway negatively regulates the phenotypic and functional maturation of monocyte-derived human dendritic cells*. Vol. 98. 2001. 2175-2182.
85. Nakahara, T., et al., *Differential role of MAPK signaling in human dendritic cell maturation and Th1/Th2 engagement.* Journal of Dermatological Science. **42**(1): p. 1-11.
86. Arce, F., et al., *Selective ERK Activation Differentiates Mouse and Human Tolerogenic Dendritic Cells, Expands Antigen-Specific Regulatory T Cells, and Suppresses Experimental Inflammatory Arthritis.* Arthritis Rheum, 2011. **63**(1): p. 84-95.
87. Segura, E., et al., *Human Inflammatory Dendritic Cells Induce Th17 Cell Differentiation.* Immunity, 2013. **38**(2): p. 336-348.
88. Lahouassa, H., et al., *SAMHD1 restricts the replication of human immunodeficiency virus type 1 by depleting the intracellular pool of deoxynucleoside triphosphates.* Nat Immunol, 2012. **13**(3): p. 223-228.
89. Berger, G., et al., *A simple, versatile and efficient method to genetically modify human monocyte-derived dendritic cells with HIV-1-derived lentiviral vectors.* Nat. Protocols, 2011. **6**(6): p. 806-816.